REDUCING ENERGY CONSUMPTION OF AIR-CONDITIONERS IN WARM-HUMID CLIMATES THROUGH DESICCANT COOLING - A CFD STUDY

BY

BISMARK BAAH

(BSc. Mechanical Engineering)

A Thesis submitted to the School of Graduate studies,

Kwame Nkrumah University of science and technology, Kumasi, Ghana

In partial fulfillment of the requirements for the degree of

MASTER OF PHILSOPHY IN MECHANICAL ENGINEERING

Department of Mechanical Engineering

College of Engineering

APRIL, 2019

DECLARATION

I hereby declare that all information in this document have been obtained and presented in accordance with academic rules and ethical conduct. I also declare that, as required by these rules and conduct, I have fully cited and referenced all material and results that are not original to this work.

Name: BISMARK BAAH

Signature:……………………………………..

This is to certify that I have read this thesis and in my opinion, it is fully adequate in quality and scope for the degree of Master of Philosophy in Mechanical Engineering.

DR. RICHARD OPOKU	……………………………..	…………………………
Main Supervisor	Signature	Date

I certify that this thesis has been assessed and has met all requirements of the University.

PROF. GEORGE Y. OBENG	……………………………..	…………………………
Head of Department (Mechanical. Engineering)	Signature	Date

ABSTRACT

The ambient temperature and relative humidity in hot-humid climates, particularly in most countries in sub-Saharan Africa, can get as high as 41 °C and 84%, respectively. For indoor thermal comfort for people, temperature of 20–25 °C and relative humidity of 50–55% should be maintained. Air-conditioners that operate with vapour compression cycle are used to maintain such conditions. In conventional Vapour Compression Systems (VCS), inlet air is cooled below its dew point for dehumidification and then reheated again to obtain air flow with desired temperature and humidity. This process of dehumidification and reheating is inefficient and leads to high consumption of energy. In Desiccant Cooling Systems, dehumidification of air is done by utilizing desiccant material to get desirable humidity and then the dry air is cooled by evaporation method or cooling coils down to suitable temperature. The process of using desiccant to control the air humidity before the air-conditioning process makes the system more energy efficient. In this work, a CFD study has been conducted to ascertain how desiccant can be used to reduce the relative humidity of air prior to the air-conditioning process. The CFD simulations were conducted using TRNSYS software with input data from the Typical Metrological Year (TMY) data for Kumasi. The results show that the desiccant system is able to reduce the cooling load of a selected inefficient VCS in an office in Kumasi by as much as 65%. In addition, analysis in this study has shown that there is potential electricity savings of 2406 kWh/year with the desiccant cooling system over the conventional VCS.

DEDICATION

I dedicate this MPhil thesis to my advisor Dr. Richard Opoku who has been very supportive throughout the entire duration of this programme. I also dedicate this work to my mum, Faustina Asantewaah for her love and prayers.

ACKNOWLEDGEMENT

I am very grateful to God for His mercy and good health throughout the period of my study. I am also grateful beyond words to my supervisor Dr. Richard Opoku for the unlimited training, support, motivation and friendship he has provided me throughout my MPhil. studies. I am much honored to have worked under his distinguished supervision over the past years, which enabled me to learn many life-time professional and personal lessons. The success of this MPhil. thesis would not have been possible without his dedication to the mission of training and empowering his graduate students to become highly qualified professionals with many opportunities open for them. I wish more scholars would follow Dr. Opoku's ethics and philosophy in training graduate students.

I also express sincerest gratitude to the director at the Brew Hammond Energy Centre, KNUST, Dr. Emmanuel Ramde for making available the software used for the simulation. This thesis would not have been possible without the help and support of many great minds and kind hearts for whom I will be indebted forever.

TABLE OF CONTENTS

LIST OF TABLES

LIST OF FIGURES

NOMENCLATURE

CPI	Control Perfect Index
DEA	Data Envelopment Analysis
HVAC	Heating Ventilation and Air-Conditioning
DCS	Desiccant Cooling System
CEH	Constant Enthalpy Humidification
CTH	Constant Temperature Humidification
LHTS	Latent Heat Thermal Storage
VCR	Vapour Compression Refrigeration
ASHRAE	American Society of Heating Refrigerating and Air-Conditioning Engineers
EES	Engineering Equation Solver
CFD	Computational Fluid Dynamics
LiBr	Lithium-Bromide
LiCl	Lithium-Chloride
PMV	Predicted Mean Vote

ADPI	Air Diffusion Performance Index
LDECAC	Liquid Desiccant Evaporative Cooling Air-Conditioning
VC	Vapour Compression
SHF	Sensible Heat Factor
LDAC	Liquid Desiccant Air-Conditioning
COP	Coe-efficient of Performance
VCCS	Vapour Compression Cooling
$\dot{M}$	mass flow rate (kg hr^{-1})
$\dot{m}$	mass flow rate (kg s^{-1})
$\dot{V}$	Volumetric flow rate (m^3 hr^{-1})
$\dot{v}$	Volumetric flow rate (m^3 s^{-1})
A	air superficial flow rate (kg m^{-2} hr^{-1} a: packing specific area (m^2 m^{-3})
ACH	air change per hour (h^{-1})
atm	atmosphere
C	Capacitance
C_p	specific heat at constant pressure (kJ kg_{-1} K_{-1}) f
	factor g: humidity ratio (kg_{water} kg_{air}^{-1})
H	enthalpy (kJ)
h	specific enthalpy (kJ kg^{-1})
h_{fg}	latent heat of evaporation (kJ kg^{-1}) L
	solution superficial flow rate (kg m^{-}_{2} hr_{-1})
P	Pressure (Pa orkPa)
Q	heat input (kJ hr^{-1}) q: cooling load (kW) T: temperature (K)

t temperature (°C) V volume (m^3)

W	Power (kJ hr^{-1})
X	solution concentration (-)
Z	dehumidifier height (m)

Greek Letters

ε	effectiveness (-)

β	regenerator temperature difference ratio (-)
ρ	Density (kg m^{-3})
γ	solution surface tension (m^{-1})
ɳ	efficiency
τ	time step

Subscripts

A air

avg average

b solution from regenerator to dehumidifier

cond condensation cs

conditioned space deh

dehumidifier equ equivalent

evap evaporation f: fresh air

i	inlet
L	solution
lat	latent
o	outlet
Reg	regenerator
s	supply air
sen	sensible
stn	standard value
u	reusing solution

CHAPTER ONE: INTRODUCTION

1.1 Background

The ambient temperature and relative humidity in hot-humid climates, particularly in most countries in sub-Saharan Africa, can get as high as 41 °C and 84%, respectively. For indoor thermal comfort for people, temperature of 20–25 °C and relative humidity of 50–55% should be maintained (ASHRAE, 2013). Conventional air-conditioning equipment which are used to provide the necessary indoor thermal comfort are therefore spreading rapidly across sub-Saharan Africa. In Ghana for instance, studies conducted (Owusu-achaw, Bimpong, 2017) estimates 10.5% annual increment in the use of air-conditioners in the country. Air-conditioners are among the major electricity consuming appliances and are dominantly used in the offices of businesses, public and commercial buildings in the daytime working hours to provide indoor thermal comfort for productive office work. It is reported that these air-conditioners consume about 60-80% (Opoku, et al, 2018), of total electricity used in the offices of public and commercial buildings in Ghana and contribute to a large extent the daytime peak demand on the national electricity grid resulting in regular grid power fluctuations.

In hot humid climates like Ghana, the high moisture content (relative humidity) of the air has huge effect on the air-conditioning load and subsequently on the electricity consumption of the airconditioning equipment. The high moisture content increases the cooling load and the electricity consumption of the air-conditioning equipment.

The aim of this work is, therefore, to determine the potential reduction of electricity consumption of air-conditioning equipment in hot-humid climates using desiccant dehumidifier during the airconditioning process.

1.2 Problem Statement

In an air-conditioning process, two main load components are associated with the conditioning of the air: (1) the air sensible load due to its temperature and (2) air latent load due to its moisture content (relative humidity). The high relative humidity of humid climate increases the latent cooling load thereby resulting in higher electricity consumption of air-conditioners.

The specific problem being investigated in this work is the high moisture content (relative humidity) of air in humid climates and how it affects the electricity consumption of airconditioning equipment.

1.3 Specific Objectives

The main goal of this thesis is to determine the potential reduction of electricity consumption of air-conditioning equipment in hot-humid climates using desiccant dehumidifier during the airconditioning process. The specific objectives are to determine:

1. the electricity consumptions of selected air-conditioners without desiccant dehumidifier.
2. analyse through computational simulations, the potential reduction of the cooling load of a given air-conditioner with desiccant dehumidifier.
3. the annual electricity saving potential of using desiccants in air-conditioning system.

1.4 Scope of Thesis

The scope of this thesis involves modelling and simulation of a desiccant air-conditioning system.

1.5 Methodology

Data on the electricity/power consumptions were collected from selected air-conditioners on KNUST Campus using Fluke 345 Data Logger. In addition, TRNSYS software was used to model and simulate the desiccant cooling concept using some selected air-conditioners at the

KNUST, Kumasi Campus, as a case study. Weather data including outdoor and indoor air conditions in terms of relative humidity and temperature were the main parameters for this study which is a Meteonorm data obtained from Type 15-6, a TRNSYS weather component.

1.6 Thesis Organization

The present thesis has been organized in five chapters. Chapter one presents the background of the thesis, the problem statement, the specific objectives, scope, and a brief summary of the methodology used for the research work. Chapter two presents a thorough literature review on airconditioning systems in general with specific emphasis on desiccant air-conditioning systems and ongoing research in this area that has helped increase energy savings. The effect of relative humidity on the energy consumption of the conventional and the desiccant air-conditioning systems are also reviewed. Chapter three presents the materials and methods used to carry out the present research work. The theoretical framework behind the problem statement is presented. The description of the analytical and numerical techniques used to solve the problem is also presented. TRNSYS, a Transient Energy Simulation System software and how it is used to analyse the present research work is presented as well. The description of the psychrometric chart and p-h diagram and their relevance to the present study and simulation of parameters for analysis in TRNSYS are presented as well. The results and discussions are presented in chapter four. Comprehensive conclusions and recommendations based on the results are presented in chapter five.

CHAPTER TWO: LITERATURE REVIEW

2.0 Introduction

This chapter presents a review of desiccant related systems that have been applied to increase energy savings in hot humid climates of the world. The two main desiccant technologies, that is, the solid desiccants and the liquid desiccants have been reviewed. Thermodynamic analysis, energy analysis, exergy analysis of the conventional vapour compression air-conditioning as well as the desiccant air-conditioning systems are also presented. The chapter concludes with the effect of relative humidity on energy consumption, and a CFD as well as TRNSYS studies on desiccant air-conditioning systems and the vapour compression air conditioning systems.

2.1 Principle of the Desiccant Cooling System

Desiccants are one subset of sorbents which attract and hold water vapour between 10% and 1100% of their dry weight (A.S.H.R.A.E Fundamentals, 2009), called desiccant capacity depending on its type and conditions. Desiccants adsorb/absorb moisture because of difference in water vapour pressure at surrounding and the surface of desiccant. This difference in vapour pressures is the driving force for the mass transfer. Desiccant material, which could be solid or liquid, attract moisture when the vapour pressure at its surface is lower than that of surrounding air until reaching equilibrium point. Some heat is released during the process and is equal to the latent heat of condensation of water plus an additional heat of dilution. The vapor pressure of air is a function of its temperature only but for desiccant it depends on temperature and concentration. Thus, for a desiccant material, capacity and vapour pressure are the two most important parameters. Figure 2.1 shows the effect of temperature and concentration on vapour pressure of Lithium Chloride (LiCl) as a liquid desiccant and Figure 2.2 displays the capacity of some desiccants for different ambient humidity conditions.

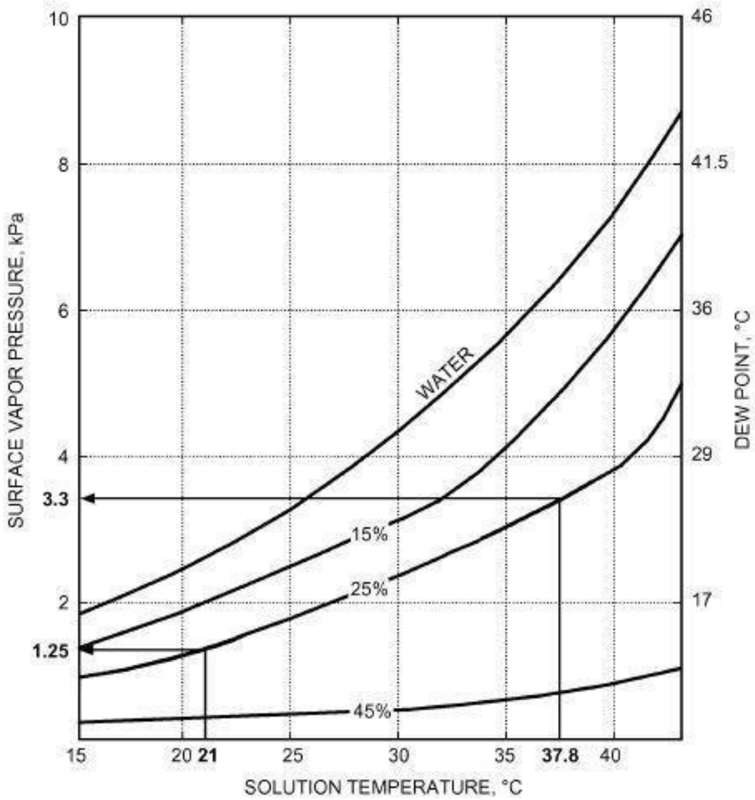

Figure 2.1 Effect of temperature and concentration on vapour pressure of LiCl

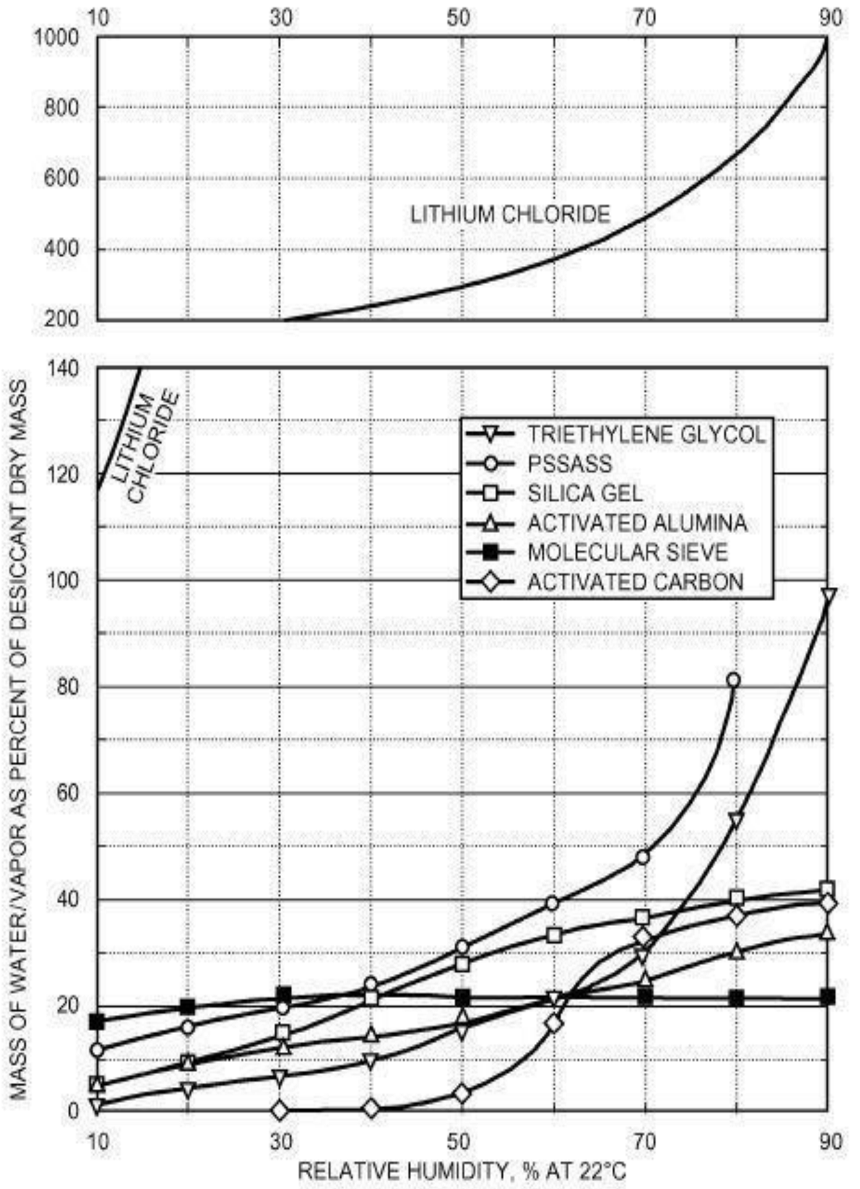

Figure 2.2 Effect of surrounding humidity on capacity of several industrial desiccants

Lower vapour pressure results in more and faster sorption process, producing air with lower humidity. Higher capacity means ability to hold more moisture at the same condition. Higher concentration and lower temperature results in lower vapor pressure of desiccant surface. Hence by increasing its temperature, attracted moisture is released, known as regeneration of weak desiccant which needs thermal energy. The sorption process is done by either absorption or adsorption. Absorption is a process in which properties of materials are changed, either physically or chemically and are usually liquid. On the contrary, in adsorption process, desiccant material is usually solid and the nature of that does not change, such as sponge soaking up water. Usually liquid desiccant (with absorption behavior) have higher capacity and lower vapor pressure compared to solid ones (with adsorption behavior). Thus, in the liquid desiccant, moisture removal rate is very high but the regeneration temperature of this type is very high. To overcome this problem, liquid desiccants are normally used in desiccant-water solution to reduce its concentration between 40 to 60%. Even though vapor pressure increases and capacity decreases in this way, regeneration temperature also drops considerably. This is due to the fact that as the concentration of desiccant goes up, regeneration temperature to bring the weak desiccant to the original state rises.

Desiccant cooling systems, firstly developed in Sweden, are novel heat driven open cycle affording an opportunity to utilize heat which might otherwise be wasted. This system consists of dehumidifying inlet air (process air) which is brought into contact with desiccant materials and then cooled down to desired temperature by evaporation or sensible cooling. In order to make the system work continuously, attracted vapor must be driven out of desiccant material by a process known as regeneration which is done by increasing material temperature. In order to be prepared for the new cycle, hot-strong material must be cooled down to be able to attract moisture again. The regeneration energy for heating is equal to the sum of:

1) Required energy to raise the temperature of desiccant to the desired magnitude

2) Required energy to vaporize the moisture, and

3) Required energy for water desorption from desiccant.

Thus, the entire the system can be divided into three main parts, namely dehumidifier, regenerator and cooling unit. The schematic working principle of basic desiccant cooling system is shown in Figure 2.3. At state 1, outside air (process air) goes through desiccant wheel called core of the system where air humidity drops significantly and temperature goes up. The air after passing through the desiccant material, is dried and also hot due to the conversion of air latent energy to sensible energy. After that, warm and dry air passes through the heat exchanger where air enthalpy drops due to reduction of temperature while humidity ratio remains constant (sensible cooling) at state 2. Air then moves toward an evaporative cooler in which water will be sprayed on the air to decrease its temperature and increase its relative humidity to appreciable levels. Note that the last process is isenthalpic, where total enthalpy remains constant. In order words, only air load changes from sensible to the latent type. The supply air goes into conditioned space and counterbalance sensible load due to heat gains and latent loads of space, which appears through mass transfer by infiltration and occupants, and finally leaves the space as return air. The return air is used to achieve two goals, as the cooler of the heat exchanger and also for regeneration of diluted desiccant material.

To fulfill the process of cooling the heat exchanger and regenerating the diluted desiccant material, the return air passes through the second evaporative cooler at step 1 as shown in Figure 2.3 to be cooled down close to dew point. After going through heat exchanger and cooling the process air, it is heated. Finally, hot air moves toward the other side of desiccant wheel where diluted desiccant is located in order to be regenerated. Hot and humid air then leaves the system to the atmosphere. Note that while the humidity ratio of air for regeneration is high because of evaporative cooling at the previous step, its impact on regeneration process is very small. Several other systems could be made with different configurations and additional components based on this system.

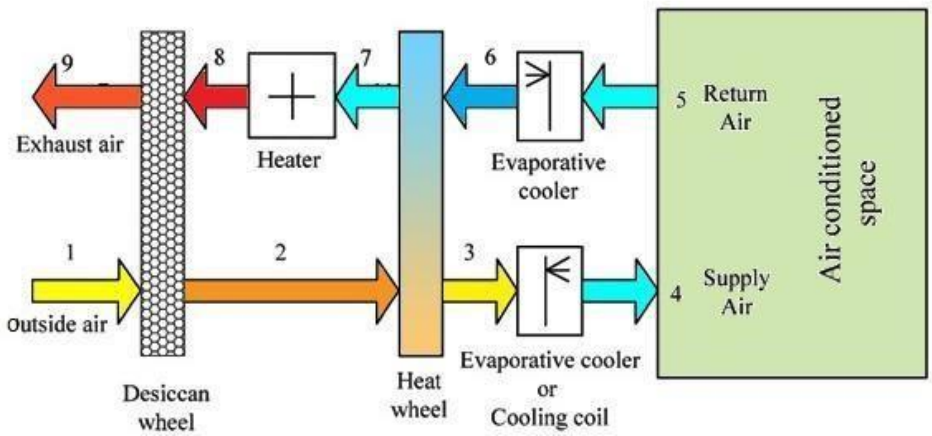

Figure 2.3 Schematic diagram of desiccant cooling system principle

2.2 Energy Saving Potential of Desiccant Air-Conditioning Systems.

Chauhan and Rajput, (2016), conducted a parametric analysis of a combined dew-point evaporative-vapour compression based air-conditioning system. They parametrically analyzed the system for a wide range of ambient temperatures and humidity ratio based on some reasonable assumptions. They also compared their system with the conventional vapour compression airconditioner on the basis of cooling load with the cooling coil working on 100% fresh air assumption. The savings of the cooling load on the coil was found to be maximum with a value of 60.93% at 46°C and 6 g/kg specific humidity. However, it was negative for very high relative humidity of ambient air [indicating that their proposed system is applicable for dry and moderate humid conditions but not for very humid conditions]. They also reported that there was an average net monthly power savings of 192.31 kWh for hot and dry conditions, and 124.38 kWh for hot and moderate humid condition.

Experimental investigation on a novel temperature and humidity independent control airconditioning system was conducted by Jiang *et al.*, 2014. The system was made up of a Solid

Desiccant Heat Pump (SDHP) to account for the latent load and a Variable Refrigerant Flow (VRF) air-conditioning system to deal with the sensible load respectively. Under cooling condition, they experimentally set up a joint SDHP and VRF system to measure the performance of the system. They also set up an experiment of widely adopted joint heat recovery ventilator (HRV) and VRF system, joint HRV and VRF system (JHVS) to compare them. They evaluated the performances of both joint SDHP and VRF system (JDVS) and JHVS. This was done by using indoor air condition, energy consumption and coefficient of performance (COP). From the experimental results, they concluded JDVS could save about 17.2% of the energy. The COP of JDVS increased by 25.7% when compared with JHVS. Furthermore, JDVS with indoor relative humidity at 50% provided better thermal comfort than JHVS.

Experimental assessment of the energy performance of a hybrid desiccant cooling system and the comparison with other air-conditioning technologies were studied by Angrisani, et al., (2015). In their study, experimental tests were used to investigate a hybrid desiccant cooling system (DCS) with desiccant wheels (DW) interacting with a small cogenerator. They analyzed the performance by varying five operating conditions; rotational speed, regeneration temperature, volume air flow rates, outdoor air temperature and humidity ratio. They also investigated numerous performance parameters based on electric, thermal and primary energy. They found out that the thermal performance of both the overall hybrid DCS and the DW reduced when regeneration temperature or flow rate increased, while electric and primary energy-based parameters rose.

Dai et al., (2015), conducted a study on the theoretical analysis, and case study on solar driven two-stage rotary desiccant cooling system combined with geothermal heat pump. Their aim was to evaluate the performance of solar hybrid air-conditioning systems using CFD simulation models based on TRNSYS. They incorporated two geothermal heat pump units with different temperatures of chilled water. This was due to the absence of solar radiation and also the fact that under-floor air supply and capillary radiation were required. They also adopted evacuated solar collectors because they integrate well with building roofs. As a demonstration project, they focused their study mainly on the performance of the solar driven Two-stage desiccant cooling (TSDC) unit and the combined operation characteristics of the hybrid air-conditioning system with geothermal heat pumps in both summer for cooling and winter for heating purposes. It was revealed that the twostage rotary desiccant cooling system was reliable and energy efficient achieving an average cooling capacity of 70 kW under typical local conditions. They also found that the solar driven TSDC unit could handle about 31.4% of the cooling load under Shanghai summer condition. Moreover, the solar driven TSDC removed about 45.3% of the moisture load. Therefore, the electric power consumption reduced to about 39.5% in comparison with conventional systems.

2.3 Thermodynamic Analysis of Air-Conditioners

Zhang et al. (2011**),** analyzed thermodynamically the air cycle refrigeration system for airconditioning Chinese train. They developed a thermodynamic system taking into account the humidity variation of a wet cycle. They used the Engineering Equation Solver (EES) software and the wet air property data to carry out a steady state simulation of the air cycle. The cycle sensitivity simulation and analysis were performed with some thermodynamic relations. They reported that the cycle pressure ratio was in the range of 2-2.5, and the cycle temperature in the range of 1-6°C. Additionally, the range of the COP was within 1-1.2.

Thermodynamic analysis of an innovative liquid desiccant air-conditioning system to supply potable water was studied by Ahmed *et al.* (2017). They compared a conventional liquid desiccant air-conditioning system with that of a proposed modified one. Their aim was to reduce the energy consumption by recovering the heat from the scavenging air using the condenser while also producing fresh water in addition to space cooling. They used Lithium chloride (LiCl) as the liquid desiccant. They established the comparison between the performance of the conventional and modified system under such given conditions as steady state, neglecting heat losses from dehumidifier, regenerator, heat exchangers or condensers. This was done by developing mathematical models for simultaneous heat and mass transfer between the condenser and the regenerator. From the generated models, they found that the modified system performance was 11.25% better than the conventional system. Also, the modified system produced 86.4 kg of fresh water per hour as a by-product under the given condition.

2.4 Exergy Analysis of Air-Conditioning Systems.

Xiao-xia et al. (2012**),** performed an exergy analysis of the energy consumption for primary return air-conditioning. They calculated the exergy loss of equipment and exergy efficiency of the system in both summer and winter. This was done by finding the exergy of heating and cooling, and the exergy of wet air. From their results, exergy efficiency in summer was greater than in winter (that is, 30.07 in summer and14.14 in winter). However, the total exergy loss was very large in winter. They obtained the highest exergy loss in the air-conditioned room in the two conditions, that is, summer and winter.

Du et al. (2015), performed a study on the operation and control in HVAC systems by the method of exergy analysis. They simulated and validated their system using real operation data. With the exergy analysis models, they developed, and evaluated the control of HVAC systems using the control-perfect index (CPI) method. They also obtained the ideal operation level of HVAC using the Data Envelopment Analysis (DEA) approach. They evaluated exergy analysis based on the

CPI method in two ways; (i) exergy comparison using the bench mark of original strategy and (ii) exergy-based CPI evaluation by using the benchmark of ideal operation. The lowest efficiency was obtained for original strategy.

Also, Ghazikhani et al. (2016), conducted an exergy analysis of two humidification process methods, that is, the Constant Enthalpy Humidification (CEH), and the Constant Temperature Humidification (CTH) in air-conditioning systems. They investigated the difference between the exergy losses (irreversibilities) and the amount of exergy consumptions and the irreversibilities of the components in the two processes. They reported that the summation of the irreversibilities in the CTH was more than that in the CEH. The power in the design condition was 12% more. They finally concluded that the CEH was superior to the CTH as a result of the less exergy consumption in the HVAC system.

An air-conditioning system incorporating thermal energy storage was analyzed with advanced exergy analysis by Mosaffa *et al.* (2014). The system comprised a combination of Latent Heat Thermal Storage (LHTS) and vapour compression refrigeration (VCR). They numerically analyzed the LHTS unit and evaluated the thermal performance of the total system using COMSOL Multiphysics and EES software respectively. They also employed an advanced exergy analysis by dividing the exergy destruction into two endogenous/exogenous and unavoidable/avoidable parts for the system. They found out that the relative irreversibility of the fan was more than the LHTS unit. Out of the overall exergy destruction rate of the system, 37.77% was unavoidable and was improved by reducing it to 36.98%. They finally concluded that all the exergy destruction of the LHTS unit was endogenous, implying that the total exergy destruction of the LHTS unit was associated with its irreversibilities.

Uçkan et al. (2014) , developed an exergy analysis process for novel configuration desiccant based on an evaporative air-conditioning system. They set up an experiment and collected data from the system during its operation. They then carried out exergy formulation on the system. From the formulation, they determined the exergy efficiency, exergy output, exergy destruction, exergy input and specific flow exergy. Additionally, they determined the components relative irreversibility and sustainability assessment. From the results, at a reference temperature of 15°C, they observed that the system's exergy efficiency was 40.7%. They also determined the exergy efficiency of the system to be between 56% and 25% for a reference temperature of 0-30. They finally concluded that the exergy analysis helped to know the theoretical upper limit of the system's performance which hitherto, could not be obtained from energy analysis alone.

2.5 Exergy Analysis of Desiccant Air-Conditioning Systems.

Hürdoğan *et al.* (2013), conducted an experiment on the exergoeconomic assessment of a desiccant cooling system. They designed, constructed and tested the system in Cukurova University, AdanaTurkey. They applied the Model and Assessment methodology outlined by Rosen and Dincer, (2003), to a novel desiccant cooling system. They evaluated the performance of the system using exergy analysis. The balanced equations were written for mass, energy and exergy flows in the system and its components as they are considered steady-state, steady-flow control volume system. Equations (2.1) to (2.4) represent the mass flow rate balance, energy rate balance, exergy rate balance and total exergy losses respectively.

$$\dot{m}\ \dot{m}_{in} \square_{out} \square \dot{m}_a \qquad \textbf{(2.1)}$$

where $\dot{m}_a$, $\dot{m}_{in}$ and $\dot{m}_{out}$ are the accumulation, inlet/input and the outlet/output mass flow rates respectively.

$$\dot{E}_{in} - \dot{E}_{out} = \dot{E}_a \qquad \textbf{(2.2)}$$

where $\dot{E}_a$, $\dot{E}_{in}$ and $\dot{E}_{out}$ represent the accumulated energy rate, inlet energy rate and outlet energy rate, respectively.

$$\dot{E}_{in} - \dot{E}_{out} - \dot{L}_{ex} = \dot{E}x_a \qquad \textbf{(2.3)}$$

$$\dot{L}_{ex} = \dot{E}x_{con} + \dot{E}x_{out\,w.} \qquad \textbf{(2.4)}$$

where $\dot{L}_{ex}$, $\dot{E}x_{con}$ and $\dot{E}x_{out\,w.}$ represent exergy thermodynamic loss rate, exergy consumption rate, and outlet exergy rate respectively.

In their experiments, flow rates of the air streams (fresh, waste and regeneration) were kept constant at 400 m^3/h. Temperature and relative humidity of the air-conditioned room were adjusted to 26 ^oC and 50% respectively according to ASHRAE comfort zone. In their calculations, the dead (reference) state values were considered as 15 ^oC and 101.325 kPa for moist air, water and refrigerant (134a). The value for the dead state humidity ratio was taken to be daily mean value of ambient air humidity ratio (0.015 kg water/kg dry air). Besides this, they conducted a parametric study at the dead state temperatures by varying the dead state temperatures from 15 to 29.43 ^oC. This enabled them to investigate the effect of the varying dead state temperatures on exergy efficiency of the system.

Using Engineering Equation Solver (EES) software package program, they found the thermodynamic properties of water and R134a. In their study, they also applied the EXCEM method to a novel desiccant-based air-conditioning system. The results assisted them in the design, improvement and optimization of the desiccant cooling system. The following concluding remarks were drawn by the study:

- The exergy efficiencies of the system decreased from 36.40% to 31.08% with increasing reference state temperatures from 15 to 29.43 ^{o}C.
- The electric heater unit was found to have the highest exergetic improvement potential rate (IP) value of 22.535 kW.
- The relative irreversibility values were 26.29%, 39.84% and 69.33 for the refrigerant unit, the heat exchangers and the whole system respectively.
- Improved potential rates and R_{ex} were in the range of 23.72-26.78 kW and 1.14-1.19 MW/USD based on the conditions and parameters considered.

2.6 CFD Studies on Desiccant Cooling

Luo, Chen, *et al.* (2016), conducted a study using CFD model on an internally-cooled liquid desiccant dehumidifier. They used the governing equations such as mass conservation, momentum conservation, species transport and energy conservation. They also developed a two-dimensional CFD model for the internally cooled dehumidifier.

They simulated the system with the CFD FLUENT software by meshing with the structured grid. They then investigated the performance of the dehumidifier under different conditions. They concluded that, a sharp increase occurred in the moisture concentration of outlet air with a parabolic trend but a linear trend occurred in the outlet air temperature when the desiccant temperature increased.

A CFD fluent software model was used to investigate the performance of a dehumidifier of a liquid desiccant air-conditioner by Luo, Yang, *et al.* (2016). They simulated the interior heat and mass transfer process with the CFD model. The basic governing equations they used were mass conservation, momentum conservation and energy conservation. After the investigation, they concluded that the dehumidifier performance worsened due to the high temperature desiccant. This was because the mass transfer driving force decreased when the contact time between the desiccant and air reduced

Luo, Yang and Lu, (2013), conducted a study of a desiccant dehumidifier. They employed the volume of fraction method, momentum equation, species equation and turbulent model. They also simulated the two-phase film flow in two-dimensional planar vertical channel from the CFD software FLUENT. They monitored three parameters, velocities of several points in the liquid film, the average mass fraction of water vapour in the moist air at the gas outlet boundary and the average temperature of moist air at the gas outlet boundary. They found that air velocity played a very vital role in the dehumidifier performance.

Longo and Gasparella, (2005), experimentally and theoretically, using CFD method, tested dehumidification and regeneration of liquid desiccant in a counter-flow random packed bed contactor with LiBr, LiCl and the new environmentally compatible salt KCOOH. They followed this by developing and verifying the theoretical model by experimental data. This was used to analyse the sensitivity of system parameters. The results showed that conventional LiCl and LiBr presented better dehumidification performance but KCOOH acted better during regeneration.

Schematic diagram of experimental setup is shown in Figure 2.4

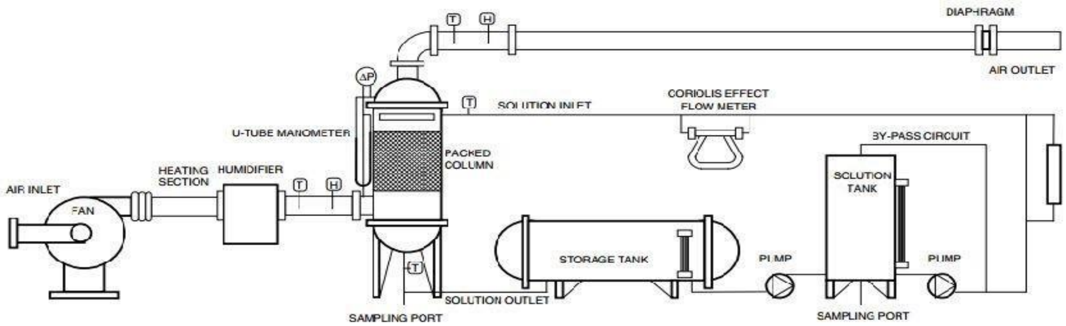

Figure 2.4 Experimental test setup

2.7 CFD Studies on Air-Conditioners

Al-waked *et al.* (2013), conducted a CFD study on the air to air enthalpy heat exchanger. They used the commercial CFD package, FLUENT to simulate the heat and moisture transfer inside the membrane heat exchanger. They also used the pre-processor GAMBIT software to develop a threedimensional CFD pressure-based solver for a steady state model of the heat exchanger. They described the water and air gas mixtures by adopting the volumetric species transport model. They then analyzed the simulation results in relation to latent effectiveness, sensible effectiveness and pressure drop across the heat exchanger's membrane. From their results, they reported that compared to the cross/ parallel flow configuration, the counter flow configuration had greater sensitivity to the distance perpendicular from the centre of the cell membrane. On the other hand, there was a minimal effect on the thermal effectiveness of the enthalpy heat exchanger for the lateral mesh length.

Aryal and Leephakpreeda, (2015), studied the thermal comfort and energy consumption effected by partitions in an air-conditioned building. They performed a CFD experiment to study the occupants' thermal comfort and energy consumption of an air-conditioned building. They used the Predicted Mean Vote (PMV) as an index of thermal comfort using a library's air-conditioned space as a case study. They measured the relative humidity using the Testo 610 handy humidity meter while the temperature and velocity were measured using the Testo 425 compact thermal anemometer. From the results of the CFD experiments, they concluded that, there was a deterioration in the thermal comfort level in some specific region when the partition was installed. This corresponded to an increase in energy consumption by 24%.

Youssef *et al.*, 2017, conducted a study for a room's comfort with cold air system using CFD model. They evaluated the performance of a cold air system inside a two-dimensional room by numerical simulation. They again studied the cold air flow at different velocities, supply and room thermal comfort. They determined the effective draft temperature from the velocity field and the temperature distribution. Also with the help of the Air Diffusion Performance Index, ADPI, they assessed the comfort level of the system and analysed independently at different loads to obtain the effect of each factor. From the results obtained, they found that comfort was not affected with the reduction in supply velocity and supply temperature. On the other hand, the ADPI was enhanced by the cooler and slower supply air.

2.8 Desiccant Technologies

An experimental investigation on the performance of radial flow desiccant bed using activated alumina was carried out by Hamed and Awad, (2011). 39.860 kg of spherical particles of activated alumina with an average diameter of 4 mm was used to form a hollow cylindrical bed with outer and inner diameters of 27.8 and 10.8 cm, respectively and length of 90 cm. During the experiments, the weight of the bed was spontaneously measured using load cell to determine the adsorbed and desorbed water during the adsorption and desorption processes, respectively. The experimental tests were carried out under different conditions of inlet air and initial bed parameters. Temperature and humidity of air at inlet and exit of the bed were measured. They presented transient variation of air conditions and the bed performance. The effect of bed pre-cooling on the system performance was studied. The results showed that air with inlet humidity ranging from 18.7 to

12.5 g/kg could be dehumidified, using activated alumina, to a lower level of humidity of 1.2 g/kg.

Zhang, et al. (2017), conducted a study on the performance analysis of a novel liquid desiccant evaporative cooling fresh air-conditioning system with solution recirculation. They established mathematical models and performance index of major components in Liquid Desiccant Evaporative Cooling Air-conditioning (LDECAC) system, that is, dehumidifier/regenerator, direct evaporative coolers and heat exchangers to simulate the whole system numerically. Based on the mathematical models, they developed flow chart for calculating the thermal performance of the whole system. They also used MATLAB software to investigate the effects of several key parameters in solution recirculation ratio (R_s), working to intake air ratio (R_a) and regeneration temperature ($T_{s,reg,in}$). They adopted an effective control method in response to the change of ambient condition and studied the effects of ambient air temperature (T_{amb}) and humidity ratio (w_{amb}) as well.

Also, based on the developed mathematical models, a parametric study on the steady-state thermal performance of LDECAC system was performed. They then investigated the performance by varying the five key parameters. The results showed that the system could handle the process air to 17.9 ^oC and 9.2 g/kg with the thermal COP of 0.56 under the designed condition. The recommended value for R_s was between 0.6 and 0.7 and that for R_a was 0.2 under the typical operating condition. The variable R_s control method was effective in response to the change of ambient air condition.

Jagirdar et al. (2017), conducted a study on the feasibility of a parallel plate desiccant coated heat and mass regenerator for dehumidification. According to the authors, the parallel plate has a significantly great Nusselt number for a relatively smaller increase in friction factor as compared to sinusoidal or hexagonal channels. They provided constant heat flux at the solid-felt interface during regeneration of the desiccant material rather than the conventional practice of heating air first and then use it to regenerate desiccant. They did this to eliminate the thermal resistance between heating source and air that would have been used to heat up the desiccant in order to regenerate it. They carried a simulation of the model using COMSOL Multiphysics. They solved for the mass, momentum, energy as well as concentration (absolute humidity) conservation equations for air domain. They used boundary conditions for the specific location (Singapore climate). Based on their numerical study, they concluded that,

- Regeneration of the desiccant was achieved by supplying heat flux directly to the desiccant material rather than heating up the air first.
- For the inlet air at 30°C with an absolute humidity of 0.019 flowing at 1.4 m/s, the average outlet humidity could be achieved.
- Parallel plate regenerator configuration could be a viable part of desiccant-based airconditioning.

Heidarinejad and Pasdarshahri, (2010), studied the effects of operational conditions of the desiccant wheel on the performance of desiccant cooling cycles. A schematic of the desiccant cooling cycle is shown in Figure 2.5. Mathematical models were used on the transient coupled heat and mass transfer to predict the performance of the system under various design and operational conditions and the numerical results were validated experimentally. Also, the effects of the regeneration temperature and rotational speed of the desiccant wheel on the COP and output cycle temperature were investigated. The optimum regeneration temperature and the rotational speed were detected and shown on the psychrometric chart in Figure 2.6.

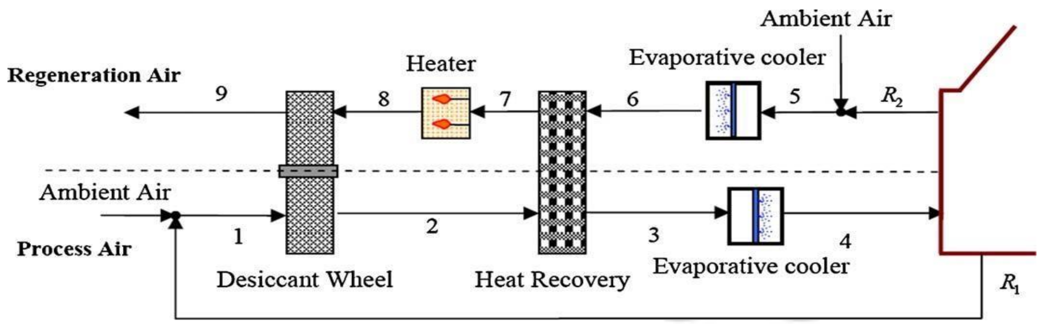

Figure 2.5 Schematic of desiccant cooling cycle

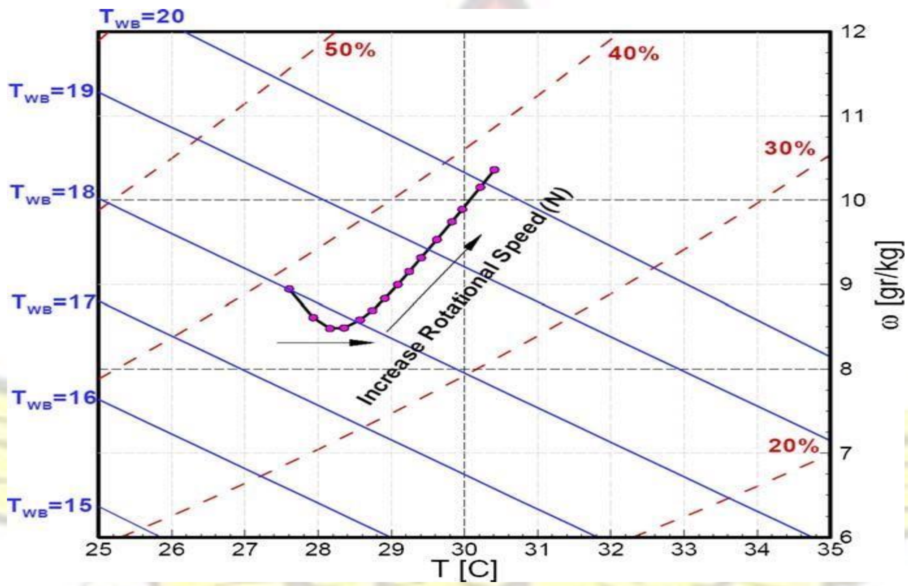

Figure 2.6. State point 3 on psychrometric chart in different rotational speeds from 0.2 to 1.6 rpm

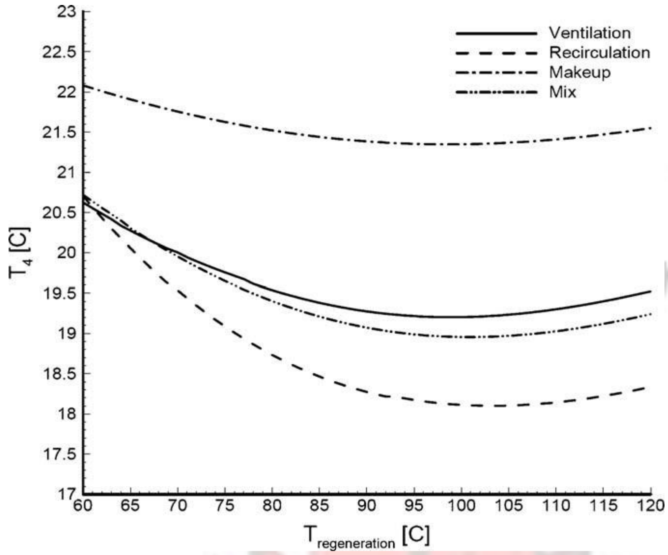

Figure 2.7. Effect of regeneration temperature on outlet cycle temperature From the results of Figure 2.6, they reported that, depending on the rotational speed of the desiccant wheel, there would be a minimum value of wet bulb temperature to be obtained. Again, from Figure 2.7, they concluded that, there was an optimum value for regeneration temperature in which the outlet cycle temperature will have its minimum value

Solar powered air-conditioning system using rotary honeycomb desiccant wheel, was studied by Kabeel, (2007). He constructed honeycomb desiccant rotary wheel from galvanized iron of 400 mm diameter and 600 mm length and clothes layer impregnated with calcium chloride solution in honeycomb form and utilised for generation and absorption processes. The temperature humidity processes of the system during absorption are shown in Figure 2.8. The regeneration constituted 33.33% of the total surface area while the absorption part equaled 66.66% of the total surface area. He measured the different parameters such as inlet and outlet air dry-bulb and wet-bulb temperatures for both absorption and regeneration processes, solar radiation intensity measured at angle of tilt at 30^{o} and air flow rate. The experimental data was obtained and specific parameters with mathematical/thermodynamic models tabulated in Table 2.1.

Table 2.1. Thermodynamic model Expressions

	$\Delta H = h_1 - h_3$	The specific cooling capacity of the supply air
	$M = m_{w1}\left(w_1 - w_2\right)$	The total moisture removal capacity of the supply air
	$M = m_w\left(w_5 - w_4\right)$	The rates of the moisture added to air by the regeneration
	$Q_c = m\,\Delta H_2$	The cooling effect of desiccant assisted air-conditioning Q_C
	$S_{COP} = \frac{2\Delta H m}{AG}$	The thermal coefficient of the system performance (SCOP)
	$\varepsilon_{ab} = \frac{w_1 - w_2}{\left(w_1 - w_2\right)_{ideal}}$	The wheel effectiveness in the absorption process
	$\varepsilon_{reg} = \frac{w_5 - w_4}{w_4}$	The wheel effectiveness in the regeneration process

Source: Kabeel, (2007).

He also obtained the results at different flow rates. From the results extracted, he arrived at the following conclusions:

- The maximum efficiency of the porous type solar air heater reached 0.6 after solar noon.
- The wheel effectiveness depended on the solar radiation and air flow rate. It approached 0.92 for the regeneration process and 0.65 for the absorption process at a flow rate of 90 kg/h
- The moisture change reached 11.5 g/kg air in the regeneration process and 74 g/kg air for the absorption process at a flow rate of 90 kg/h.

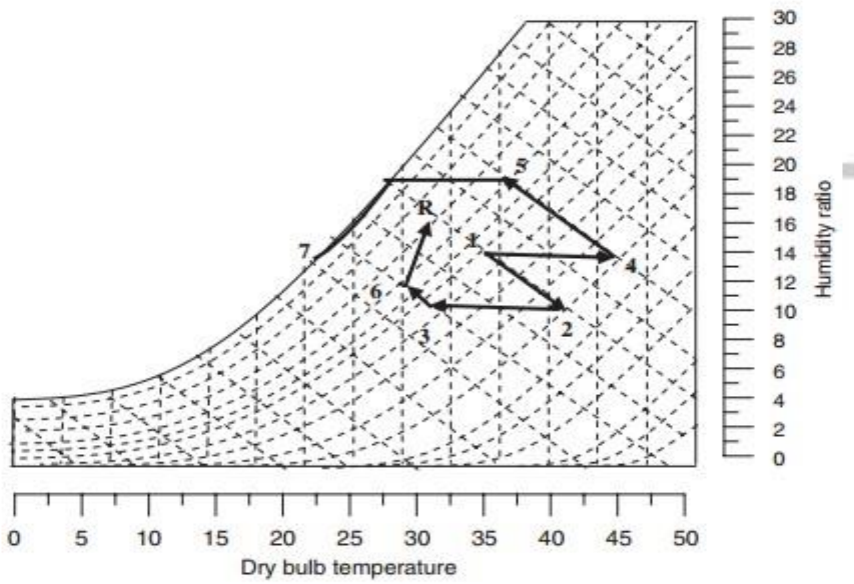

Figure 2.8. Psychometric chart of the system processes

Performance study of solid desiccant vapor compression hybrid air-conditioning system was experimentally carried out for typical hot and humid weather of Roorkee by Jani et al. (2016). The overall system performance was evaluated for a cooling season from March to mid-October on the basis of various outdoor conditions. It was found that the system could achieve a good performance in hot and humid climatic conditions due to significant reduction in the humidity ratio of the process air from 18.5 g/kg dry air to 7.10 g/kg dry air when it passes through the rotary desiccant dehumidifier. It was also found that the hybrid cooling system highlights good performance in hot and humid climatic condition. The system ensured 61.7% reduction in process air humidity ratio at the outlet of the desiccant wheel as compared to outdoor humidity ratio. The effect of variations in outdoor temperature on dehumidifier performance was featured as well. The results obtained also showed that the system performance is highly sensitive to the change in outside ambient condition. In addition, Jia *et al.* (2006), experimentally tested a hybrid desiccant air-conditioning system to control the humidity. It was found that, compared with the conventional VC (vapor compression) system, the hybrid desiccant cooling system saved 37.5% electricity when the process air temperature and relative humidity were maintained at 30°C, and 55% respectively. It was also found that the sensible heat factor (SHF) of the evaporator cooling coil increased significantly. Hence, most of the evaporator surface of the hybrid desiccant system remained dry during the operating period. Thus, subsequent reheat was avoided and the electric power consumption of the hybrid desiccant system was reduced.

The design of the conditioner regenerator can greatly affect its ability to absorb/desorb moisture and heat. The two main types of desiccant systems are packed bed and falling film, each with its advantages and disadvantages. In a comprehensive review of liquid desiccant technologies Mei and Dai, (2008), presented research in areas including desiccant and packing materials, conditioner flow patterns, regeneration models and energy storage. Their research identified packed-bed heat and mass exchangers as the most commonly researched exchanger structure and lithium bromide, lithium chloride and tri-ethylene glycol as the most widely used single desiccants.

In a survey of hybrid liquid desiccant air-conditioning systems, Mohammad *et al.* (2013), described a variety of hybrid systems and compared them to vapour compression systems. It was found that the application of hybrid systems in hot and humid climates significantly reduced the size and power required of the vapour compression unit. This is due to the Liquid Desiccant Airconditioning system (LDAC) taking over the large latent cooling load. The literature discussed showed an increase in COP and energy savings of 23.1% – 73.8% and 26% – 80% respectively, when using a hybrid system over a conventional vapour compression system.

CHAPTER THREE: MATERIALS AND METHODS

3.1 Problem Formulation

There are two types of loads that an air-conditioning system has to meet (sensible and latent). The sum of these two is the total load. Sensible load is as a result of heat transfer due to temperature difference. Latent load on the other hand is as a result of generated moisture (relative humidity) and mass transfer

In conventional Vapour Compression Cooling Systems (VCCS), the process air has to be cooled below its dew point to remove latent load by condensation and then be reheated to meet suitable temperature. Energy demand for reheating after condensation goes up. This makes the conventional VCCS systems less energy efficient and is responsible for the high energy consumption.

However, desiccant cooling systems are able to reduce relative humidity, thereby contributing significantly in the overall energy savings of air-conditioners. In the Desiccant Cooling Systems, condensation occurs without any dependence on temperature and therefore no need for reheating. This results in lower energy demand even at high ambient air relative humidity compared to any other system.

The objective of this work is therefore to estimate the potential savings in electricity consumption in using desiccant cooling system to reduce the overall air-conditioning load.

The first phase of this work was to measure the power consumption of some selected conventional air-conditioners and use the information in the analysis of the electricity savings potential with the desiccant cooling system.

3.2 Data Measurement on the Conventional Air-Conditioners

Data was collected from selected air-conditioners at the KNUST, Kumasi Campus to determine the power consumption. This was done using Fluke 345 energy clamp meter which measures the power consumption, power factor, voltage and current.

The Fluke 345 clamp meter can record data without any interference with the electrical wiring of the air-conditioners. It is also able to measure data at intervals of one second, two seconds, five seconds, minutes, etc. over a certain number of hours, days weeks or even months. Figure 3.1 shows the connection of the clamp meter and sample reading from the screen. Since one of the objectives of this work is to determine the actual electricity consumption of some selected airconditioners, the main parameters considered were the power consumption and the duration for each reading in seconds. From these parameters, the energy consumption (E) was determined from

$$E = \int_0^T W_c \, \Delta t \qquad \textbf{(3.1)}$$

where W_c represents the instantaneous power consumptions during the period of measurement, Δt is the time step used to take the readings of the air conditioner's power consumption and T is the period. The time step used in this research was two seconds. For any given time step, the energy consumption of each air-conditioner was determined. The Fluke 345 clamp meter can also measure other information such as AC and DC Voltage and Current of both single and 3-phase systems, reactive power, active power, and power factor.

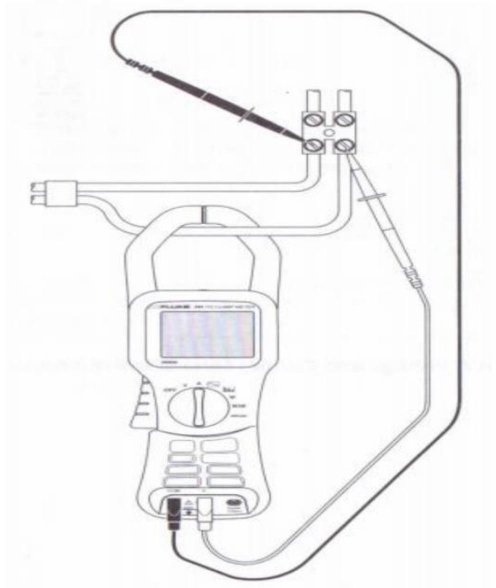

(b)

Figure 3.1 Connection of the clamp meter and sample reading from the screen

The data collected was analysed in MATLAB and compared with the information provided on the name plate. The name plate data was taken from the installed air-conditioners at the selected locations. This provided the energy consumption per year, Energy Efficiency Rating (EER) etc.

3.3 Set-up for Power Consumption Measurement

Figure 3.2 shows the set-up used for the measurement of the actual data of the various airconditioners. The data was collected over a period of 8 hours for three consecutive days for each air-conditioner. The data obtained after each day was transferred to a computer before the start of a new data collection. The fluke 345 clamp meter has four storage locations. During data collection, the storage location named 1-2-3 was used to store the data since it has the largest storage capacity. Also, the data can be viewed in real time on the screen during the measurement. After the measurement, measured data from the four different air-conditioners were then analysed in MATLAB. The results obtained are presented and discussed in chapter four.

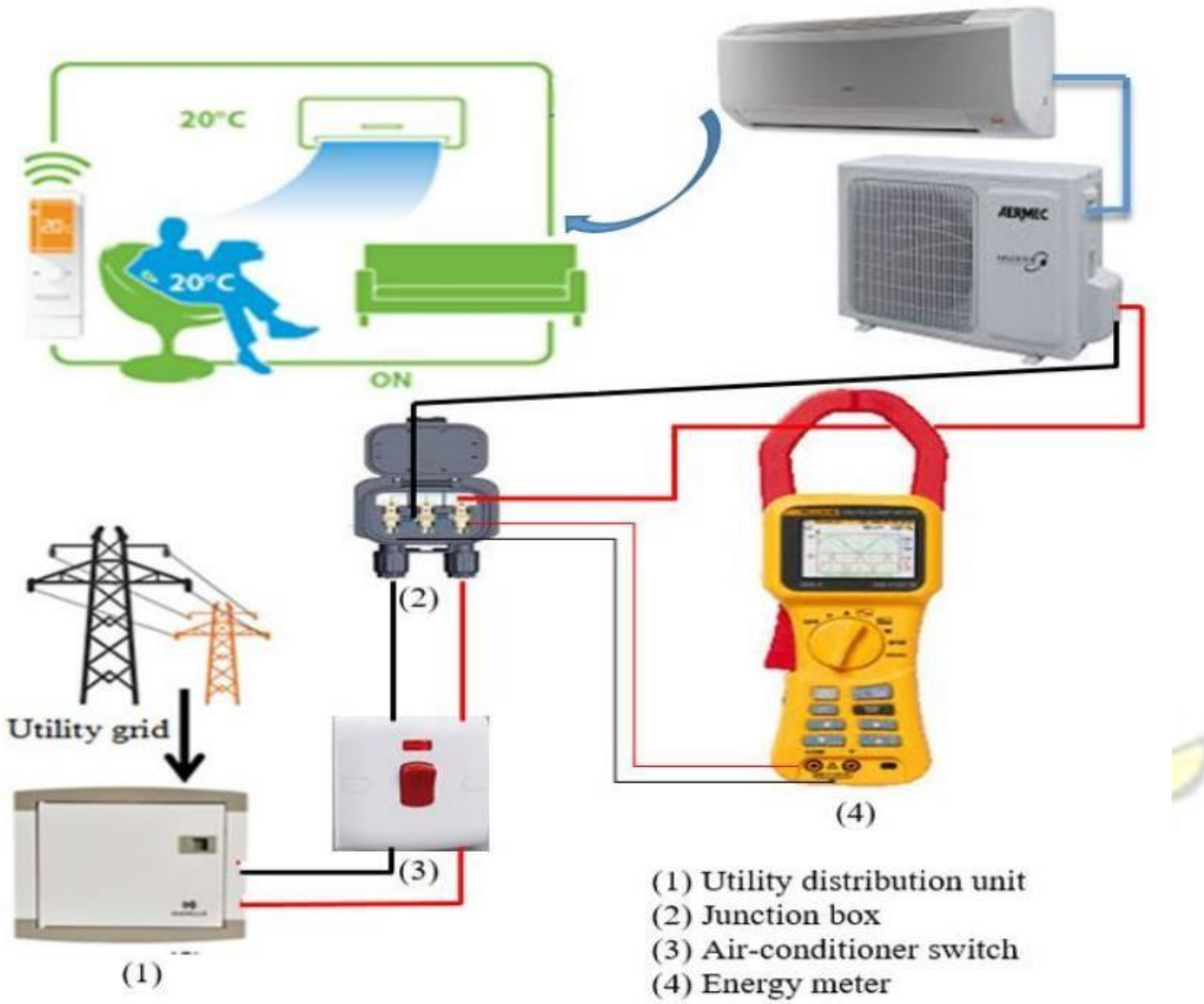

Figure 3.2 Experimental set-up used for the measurement of the power consumption of the air-conditioners

3.4 CFD Study

3.4.1 Climatic Conditions

Kumasi is located at 6° 40´N and 1° 37´W at an altitude of 250 m and approximately 500 km away from the equator. The tropical climate in Kumasi accounts for its high humidity and corresponding temperature throughout the year, whereby there is a difference between the rainy and dry seasons. Table 3.1 presents the monthly mean temperature, precipitation and relative humidity of Kumasi

Table 3.1: Monthly mean temperature, precipitation and relative humidity of Kumasi for a period of 10 years.

	Temperature °C		Precipitation		relative	Sunshine Hours
	max. Ø	min. Ø	mm	days	**humidity**	h/day
Jan	31	19.6	24	1	72	6
Feb	32.6	21	65	5	69	6.6
March	32.2	21.7	143	8	73	6.6
April	31.8	21.8	149	9	75	6.8
May	30.8	21.9	201	13	78	6.6
June	29.2	21.5	224	15	81	4.9
July	27.6	21	139	10	82	3.3
Aug	26.9	20.6	83	9	83	2.5
Sept	28.4	21.1	159	14	81	3.5
Oct	29.8	21.2	192	14	80	5.2
Nov	30.8	21.1	100	8	77	6.5
Dec	30.5	20.5	30	2	77	5.7
Year	**30.1**	**21.1**	**1509**	**108**	**77**	**5.3**

Source: Wetterkontor.de

3.4.2 Determination of the Cooling Load

In order to find the required cooling capacity of the air-conditioning system, one has to take into account the sensible and latent loads due to ventilation, and leakage losses in the return air ducts. Equations (3.2) and (3.3) give the equations used for the determination of the cooling loads.

$$Q_{sen} = \dot{m}(1-X)c_{p,m}(T_o - T_i) = \dot{V}\rho_o(1-X)c_{p,m}(T_o - T_i) \qquad \textbf{(3.2)}$$

where $\dot{m}$ and $\dot{V}$ are the mass and volumetric flow rates of the ventilated air and X is the by-pass factor of the coil

$$\dot{Q}_{lat} = \dot{m}(1-X)h_{fg}(W_o - W_i) = \dot{V}\rho_o(1-X)h_{fg}(W_o - W_i) \quad \textbf{(3.3)}$$

where W_o and W_i are the humidity ratios of the ambient and conditioned air, respectively and h_{fg} is the latent heat of vaporization of water. The total cooling load is obtained by summing the sensible and latent loads as shown in equation 3.4.

$$\dot{Q}_{total} = \dot{Q}_{lat} + \dot{Q}_{sen}$$

(3.4)

3.4.3 Transient System Simulation Tool (TRNSYS)

A. Dehumidifier and Regenerator Model

Since liquid desiccant dehumidifier and regenerator mathematical models are neither available in TRNSYS nor TESS library, their models are adopted from literature and incorporated into TRNSYS for the analysis.

There are three main mathematical modeling methods for contactors (dehumidifier and regenerator): 1) computational fluid dynamics model (CFD); 2) number of transfer units (NTU); and 3) fitting algebraic equation. Out of these mathematical models, the CFD is the most exact one and the algebraic equation is the least exact model. However, the algebraic equation is adopted here because analysis of a finite difference model is very complex and iterative numerical solutions are required. Hence, algebraic equations are adopted which are simple equations used for quick prediction of moisture effectiveness (ε) with the aim of determining air outlet properties using Equation. (3.5) and Equation. (3.6). Note these two equations explicitly show that the contactor effectiveness is a function of the humidity ratio (g) and enthalpy (h) of the inlet air (subscript A,i) and its equilibrium state (subscript A,equ) streams.

$$g_{A,o} = g_{A,i} - \varepsilon_g \left(g_{A,i} - g_{A,equ} \right) \quad (3.5)$$

$$h_{A,o} = h_{A,i} - \varepsilon_h \left(h_{A,i} - h_{A,equ} \right) \quad (3.6)$$

where $g_{A,equ}$ is the humidity ratio of air when it is in equilibrium with inlet solution, meaning that water partial pressure of air is equal to vapour pressure of inlet solution. Similarly, $h_{A,equ}$ is obtained when air temperature and humidity ratio are equal to inlet solution temperature and vapour pressure respectively. Using this set of equations, air outlet humidity ratio and enthalpy are obtained if dehumidification and enthalpy effectiveness of dehumidifier are known and subsequently, the air outlet temperature.

While the accuracy of the method is slightly lower compared to finite difference, it is still acceptable for some applications such as air-conditioning and in fact their simplicity is beneficial as it enables hourly system analysis in a reasonable amount of time. Algebraic equations are obtained through curve fitting of the available input and output data of dehumidifiers and regenerators, either using experimental tests or finite difference results. Unfortunately, this type of information is rare and only a handful of such studies are available in the open literature.

i. Dehumidifier

Martin and Goswami, (2011), developed correlations for dehumidification and enthalpy effectiveness, obtained from Oberg and Goswami, (1998) and shown in Equations (3.7), and (3.8), of a counter-flow random packed bed dehumidifier for lithium chloride (LiCl).

$$\varepsilon_g = 1 - C_1 \left(\frac{S}{A} \right)^a \left(\frac{h_{A,in}}{h_{S,in}} \right)^b \left(aZ_t \right)^c \quad (3.7)$$

$$\eta_h = 1 - C_1 \left(\frac{S}{A}\right)^{a} \left(\frac{h_{S,in}}{h_{A,in}}\right)^{b} \left(a_t Z_t\right)^{c} \quad (3.8)$$

Where,

$$a_t = k_1 \left(\frac{S}{c}\right) + m_1 \quad (3.9)$$

$$c = k_2 \left(\frac{S}{c}\right) + m_2 \quad (3.10)$$

Here, C_1, b, k_1, k_2, m_1, and m_2 are the constants adopted from Martin and Goswami, 2011, and shown in Table 3.2 through fitting the correlation to experimental data. These constants are substituted in Equations (3.7) and (3.8) to give

$$\eta_g = 1 - 148.3 \left(SA\right)^{0.396 - \frac{1.57}{0.029}} \left(h_{S,in} h_{A,in}\right)^{-0.751} \left(a Z_t\right)^{0.0331 \, 0.029 - 0.906} \quad (3.11)$$

$$\eta_h = 1 - 13.77 \left(SA\right)^{0.289 \, 0.029 - 1.12} \left(h_{S,in} h_{A,in}\right)^{0.528} \left(a Z_t\right)^{0.0044 \, 0.029 - 0.365} \quad (3.12)$$

Table 3.2. Constants for performance correlations

	C_1	B	k_1	m_1	k_2	m_2

E_g	48.3	−0.751	0.396	−1.57	0.0331	−0.906
E_h	3.77	−0.528	0.289	−1.12	−0.0044	−0.365

Also from the research by Ge et al. (2011) the rate of dehumidification is easier to control by controlling the solution temperature rather than the concentration. The desired amount of moisture to be removed/absorbed in the condensation can be obtained from,

$$\dot{M}_{A,o} = \dot{M}\left(\frac{1+g_{A,i}}{1+g_{A,o}}\right) \qquad \textbf{(3.13)}$$

Once the air outlet humidity, enthalpy and other temperatures are known, other outputs can be obtained through mass and energy balance equations for the dehumidifier, Equations (3.14) to Equation (3.17) For the solution:

$$\dot{M}_{L,o} = \dot{M}_{L,i} + \dot{M}_{cond} \qquad \textbf{(3.14)}$$

$$X_{L,o} = \frac{\dot{M}_{L,i} X_{L,i}}{\dot{M}_{L,o}} \qquad \textbf{(3.15)}$$

$$h_{L,o} = \frac{\dot{M}_{L,i} h_{L,i} + \dot{M}_{A,i} h_{A,i} - \dot{M}_{A,o} h_{A,o}}{\dot{M}_{L,o}} \qquad \textbf{(3.16)}$$

And for air

$$\dot{M}_{A,o} = \frac{\dot{M}_{A,o}\left(1+g_{A,i}\right)}{1+g_{A,o}} \qquad \textbf{(3.17)}$$

ii. Regenerator

As there exists no algebraic model for regenerator effectiveness at open literature, Gandhidasan (2005) theoretical study is used to model the regenerator as seen in Equation (3.18) (calculates superficial water evaporation rate from solution in the dehumidifier. This general model which may be applied to any regenerator without emphasis on its type and operating conditions, requires outlet air temperature of regenerator, to obtain the value of regenerator temperature difference, ε.

Thus, it is to be used in accordance with experimental data.

$$\dot{M}_{evap} = \frac{1}{h_{fg}}\left[\dot{Q} - \dot{M}_A C_{pA}\left(T_{L,i} - T_{A,i}\right)\varepsilon\right] \qquad \textbf{(3.18)}$$

Where,

$$\varepsilon = \frac{T_{A,o} - T_{A,i}}{T_{L,i} - T_{A,i}} \qquad \textbf{(3.19)}$$

3.4.4.1 Description of the TRNSYS Software

The system was modeled in TRNSYS, a transient simulation program used to iteratively solve complex thermal systems. The software allows the use of defining parameters to characterize individual components. These components are then connected to each other in the desired configuration through a series of inputs and outputs. When a full system model has been built, TRNSYS assembles the applicable order of operations into a control deck which is used by the numerical equation solver. The TRNSYS software package includes a large library of preprogrammed components, called “Types”, including heat exchangers, boilers and heat-pump models. Additionally, the TRNSYS software allows the user to develop and add custom components for increased flexibility. Each Type is made up of three main items known as windows. These are “Parameter”, “Input” and “Output”. The window showing Parameter contains constant physical characteristics of that component and provides users to specify these constants. Figure 3.3 illustrates the window parameter of a Desiccant/ Dehumidifier (Type 716) with constant properties such as Design Regeneration Air Inlet Humidity Ratio/Temperature and Design Process Air Inlet/Outlet Temperature and can be edited. Window Parameter of other Types/components are shown in Figure 3.4 and Tables 3.3 and 3.4.

Table 3.3 Parameter window sample of the Dehumidifier/ Desiccant

Name	Value	Unit
Humidity Mode	2	-
Design Process Air Inlet Temperature	28	□C
Design Regeneration Air Inlet Temperature	50	□C
Design Process Air Outlet Temperature	45	□C
Design Process Air Inlet Humidity Ratio	0.008	Fraction
Design Regeneration Air Inlet Humidity Ratio	0.01428	Fraction

Table 3.4 Input window sample Dehumidifier/ Desiccant

Name	Value	Unit
Process Air Inlet Temperature	30	□C
Process Air Inlet Humidity Ratio	0.007	-

Process Air % Relative Humidity	99.0	% (base100)
Process Air Inlet Flowrate	1000	Kg/hr
Process Air Inlet Pressure	1.00	Atm
Process Air Pressure Drop	0.01428	Atm
Regeneration Air Inlet Temperature	71	°C
Process Air Humidity Ratio	0.01428	-

The present work used custom components to model the conditioner, regenerator and desiccant system. In addition, the Thermal Energy System Specialists (TESS) has developed several components for equipment that are not included in the standard TRNSYS deck. Table 3.5 lists the components that are used to model the AC systems investigated in this study.

Table 3.5 Modelled components of the Desiccant AC System

Type	Parameter	Type	Parameter
	Building model	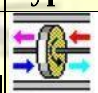	Heat wheel
	TMY2 weather data	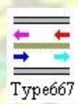	Energy recovery ventilator
	Pump	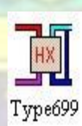	Sensible heat exchanger
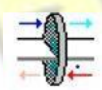	Desiccant/ Dehumidifier		Evaporative cooler
	Psychometric relations		Stratified storage tank
	Output recorder		Solar thermal collector

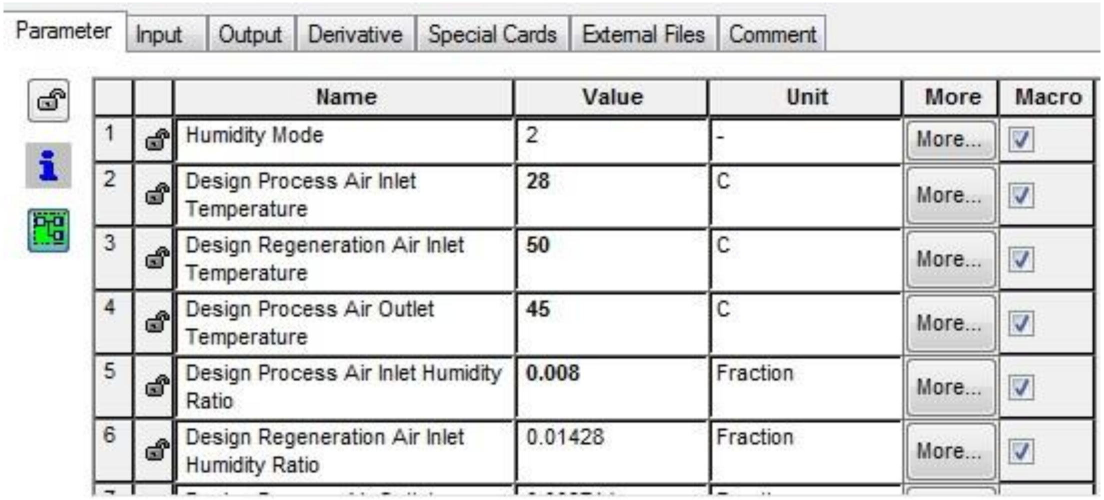

Parameter | Input | Output | Derivative | Special Cards | External Files | Comment

		Name	Value	Unit	More	Macro
1		Humidity Mode	2	-	More...	☑
2		Design Process Air Inlet Temperature	28	C	More...	☑
3		Design Regeneration Air Inlet Temperature	50	C	More...	☑
4		Design Process Air Outlet Temperature	45	C	More...	☑
5		Design Process Air Inlet Humidity Ratio	0.008	Fraction	More...	☑
6		Design Regeneration Air Inlet Humidity Ratio	0.01428	Fraction	More...	☑

Figure 3.3 Parameter window sample of the Desiccant/Dehumidifier

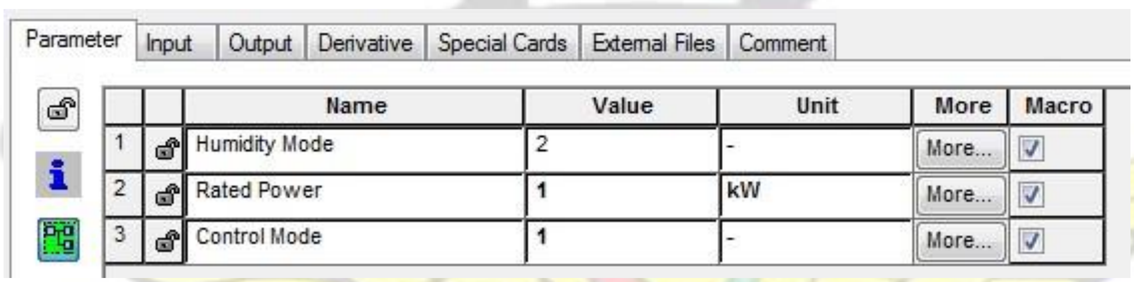

Parameter | Input | Output | Derivative | Special Cards | External Files | Comment

		Name	Value	Unit	More	Macro
1		Humidity Mode	2	-	More...	☑
2		Rated Power	1	kW	More...	☑
3		Control Mode	1	-	More...	☑

Figure 3.4 Parameter window sample of the Evaporative Cooler

Next to the parameter is the input window which shows the required input for a particular Type and can also be the output of other types/components. Figure 3.5 displays the input window for desiccant/dehumidifier (Type 716). Inputs which are not connected are (have blue names at input window) constant at specified values. Correspondingly, the output window displays possible/available output from a component/Type which may be linked to another Type as their outputs. Figure 3.6 shows the output window for Type 716.

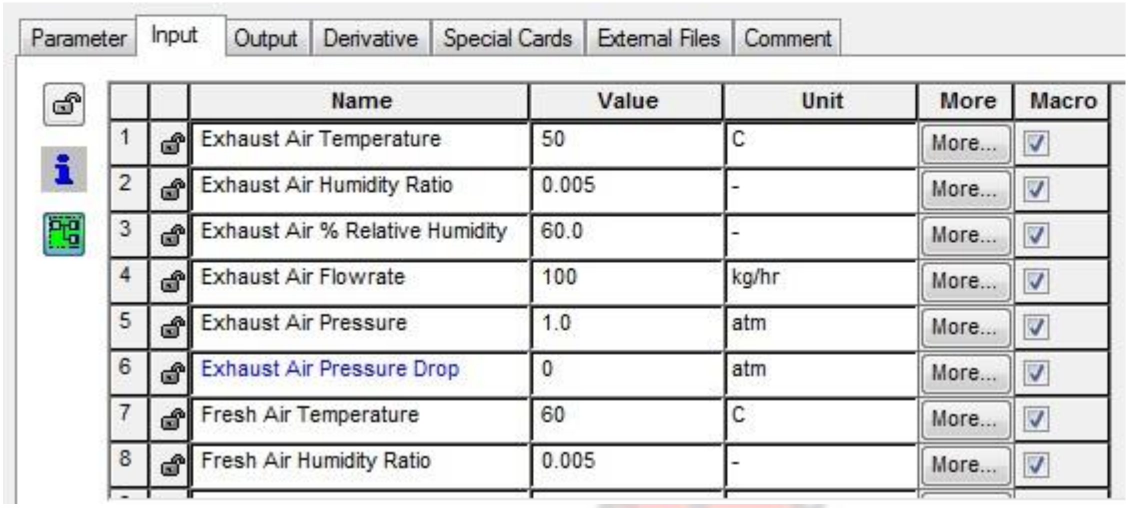

Figure 3.5 Input window sample of the Desiccant/Dehumidifier

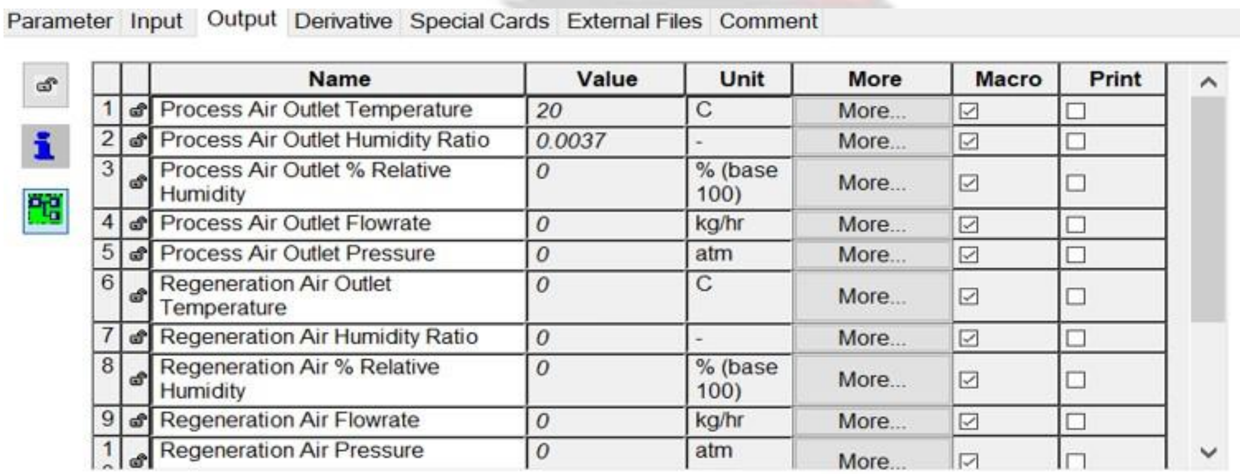

Figure 3.6 Output window sample Model of the Desiccant/Dehumidifier

In simulating the operation of the model, an important step is to specify the values of transient variables between the output(s) of one component/Type to input(s) of another Type. This is done so that information flow can readily occur by using a link between two components. The user should use graphical user interface (GUI) to specify the details of other links between the two components. This is opened by double-clicking on the link as shown in Figure 3.7. To specify the link between two Types/components, the user connects the outputs of the first Type which is on the left-side to the inputs required of the second Type/component which is shown on the rightside.

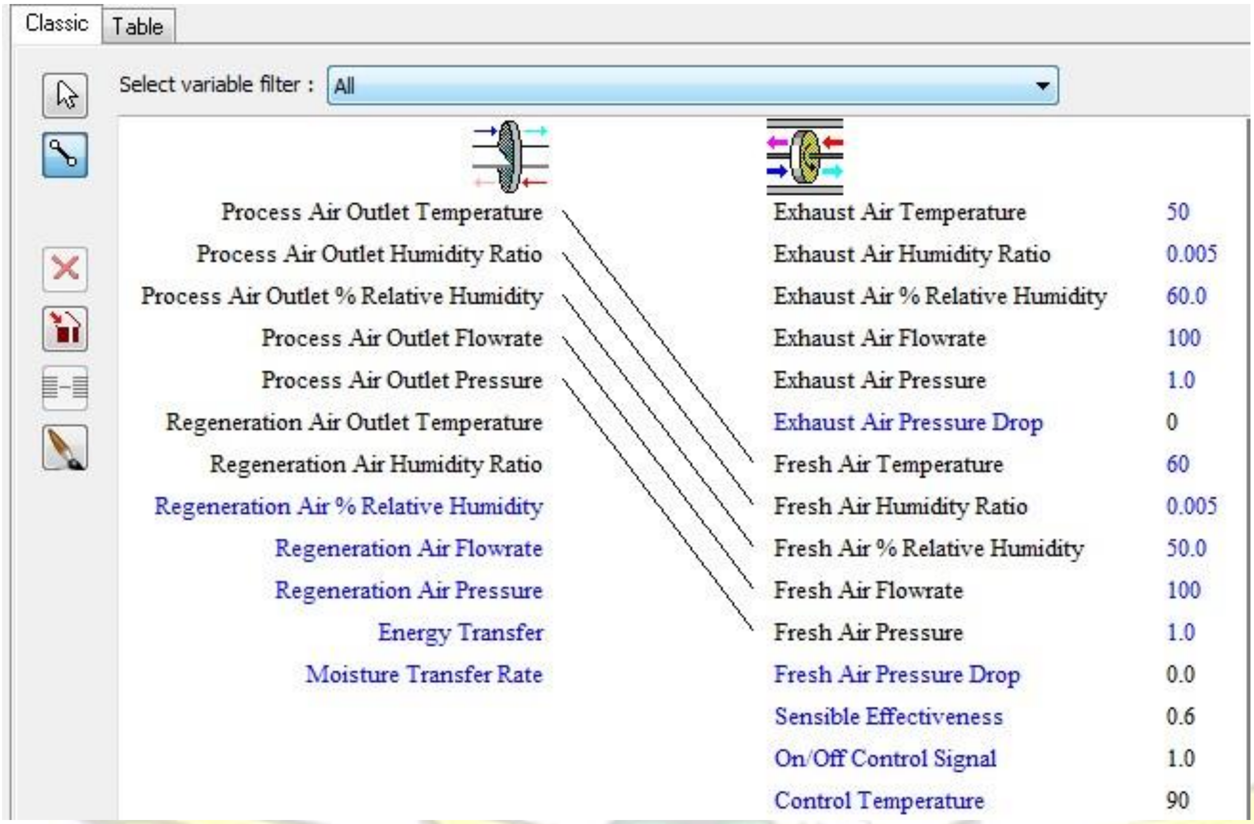

Figure 3.7 Sample connection window between desiccant wheel and heat wheel Figure 3.8 demonstrates current work TRNSYS model where Types and information flow are demonstrated by icons and links between them respectively.

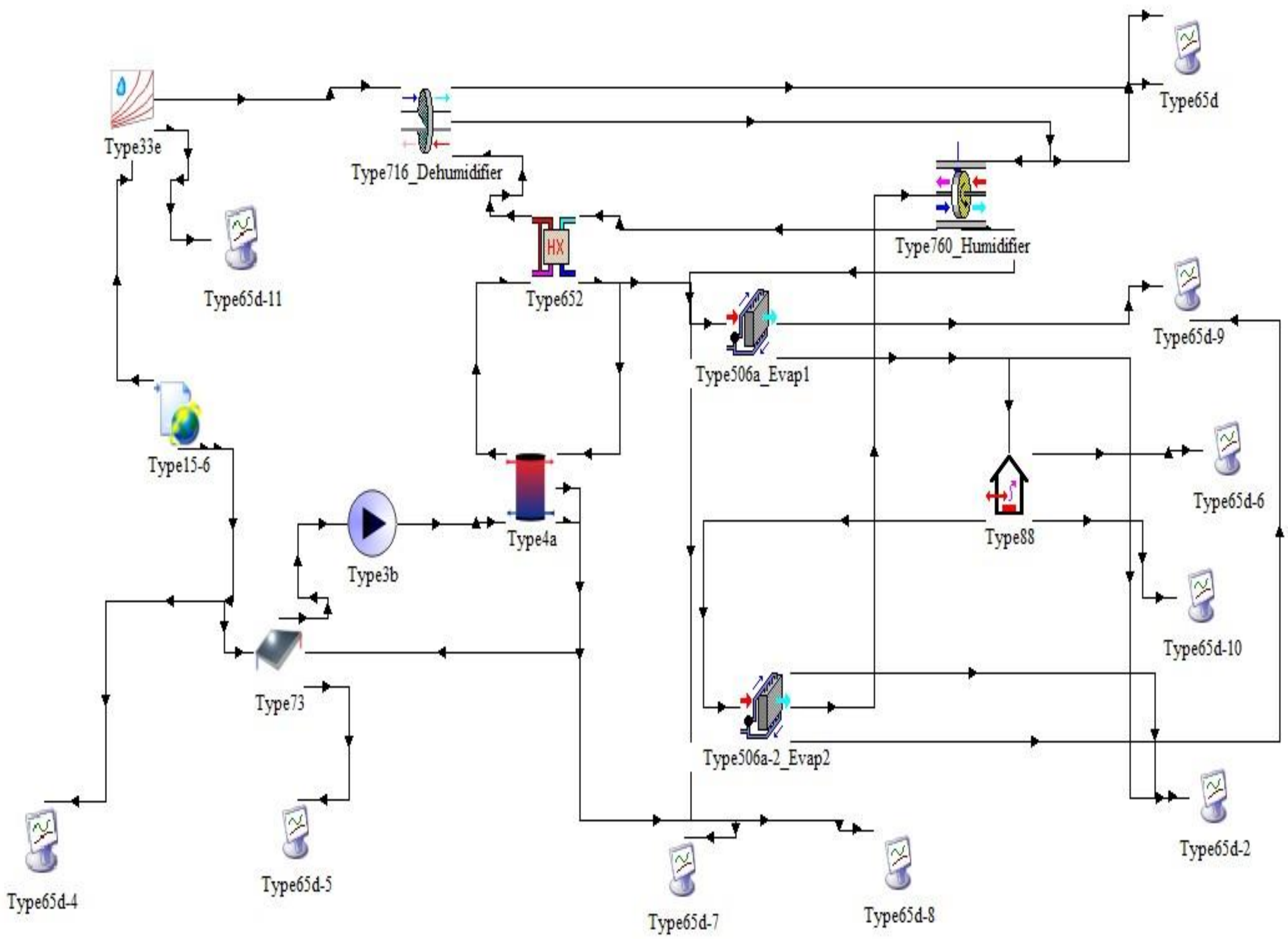

Figure 3.8 TRNSYS diagram of the Desiccant Cooling System

The results of the experiments conducted and the TRNSYS simulations are presented in the next chapter (chapter four) of this thesis.

CHAPTER FOUR: RESULTS AND DISCUSSIONS

This chapter presents the results obtained from this work. First, the result obtained from the analysis of the measured power consumption of the selected air-conditioners at KNUST campus are presented and discussed. Also, the results of the comparison of the average measured power consumption with name plate of the selected air-conditioners are discussed. Additionally, the TRNSYS simulation of the desiccant air-conditioning system results are presented in this chapter.

4.1 Power Consumption of four Selected Air-Conditioners

A plot of the measured power consumption against time for some selected conventional airconditioners without desiccant at the College of Engineering, KNUST are displayed in Figure 4.1 to Figure 4.4.

4.1.1 Split-type Inverter Air-Conditioner (Aermec A/C)

Figure 4.1 shows a graph of the power consumption against time of the Aermec split-type airconditioner.

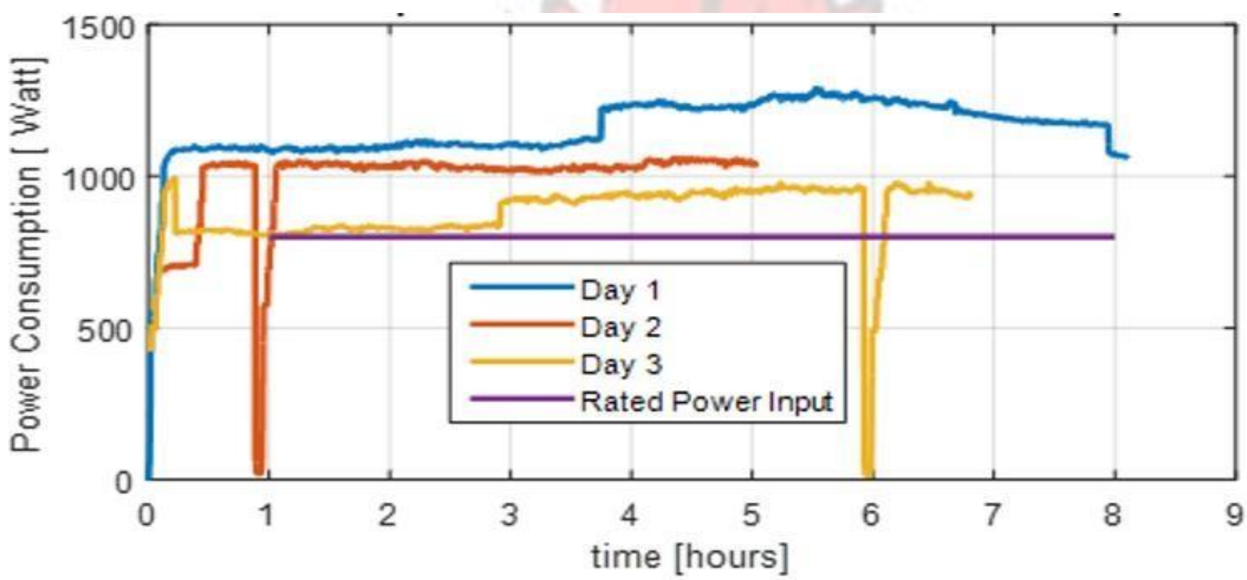

Figure 4.1 Power consumption of Aermec air-conditioner over a three day period

In Figure 4.1, the power consumption of the Aermec inverter type air-conditioner is measured to obtain the actual power consumed. This is done for three consecutive days. Day one recorded the highest power consumption of about 1250 W with 900 W being the lowest. The overall measured average power consumption during the period is about 1020 W.

4.1.2 Window-type Air-Conditioner (White-Westinghouse)

The measured power consumption of Window type air-conditioner located at the solar lab at the College of Engineering, KNUST is shown in Figure 4.2.

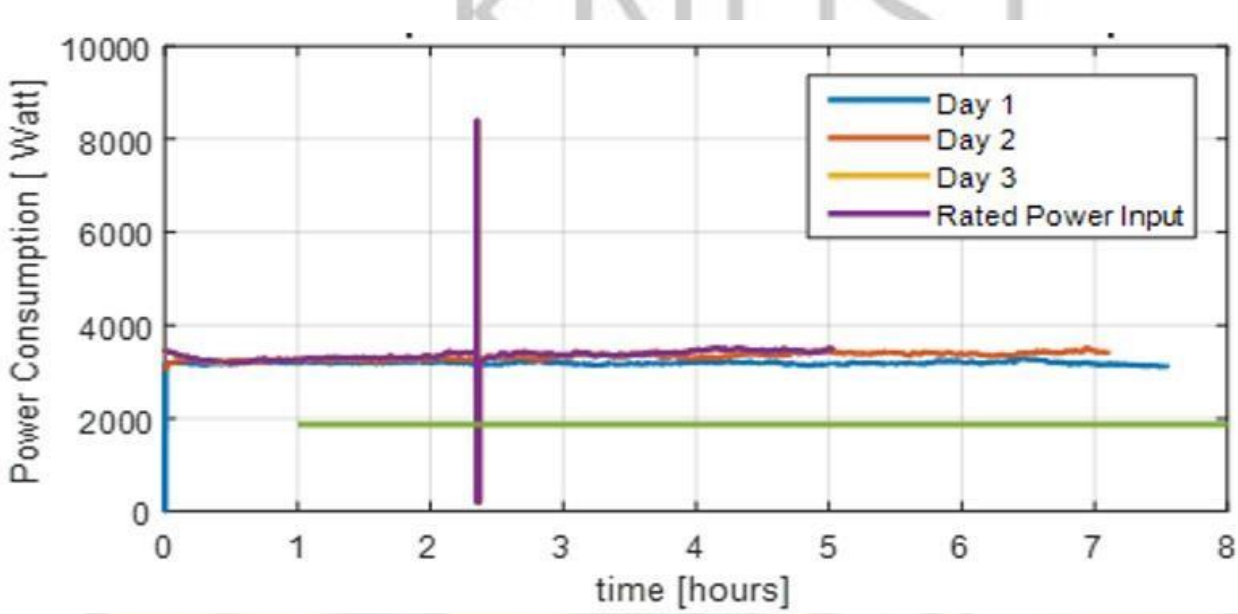

Figure 4.2 Power consumption of window type air-conditioner over a period It is observed that the maximum power consumption measured is 3550 W and that for the minimum is about 3350 W. Power of 3500 W is obtained as the average measured power consumption during the entire period.

4.1.3 Split-type conventioneer air-conditioner

From Figures 4.3 and 4.4, variation of the measured power consumptions of both the Metrology lab and the MSc. Mechanical Lecture room are shown.

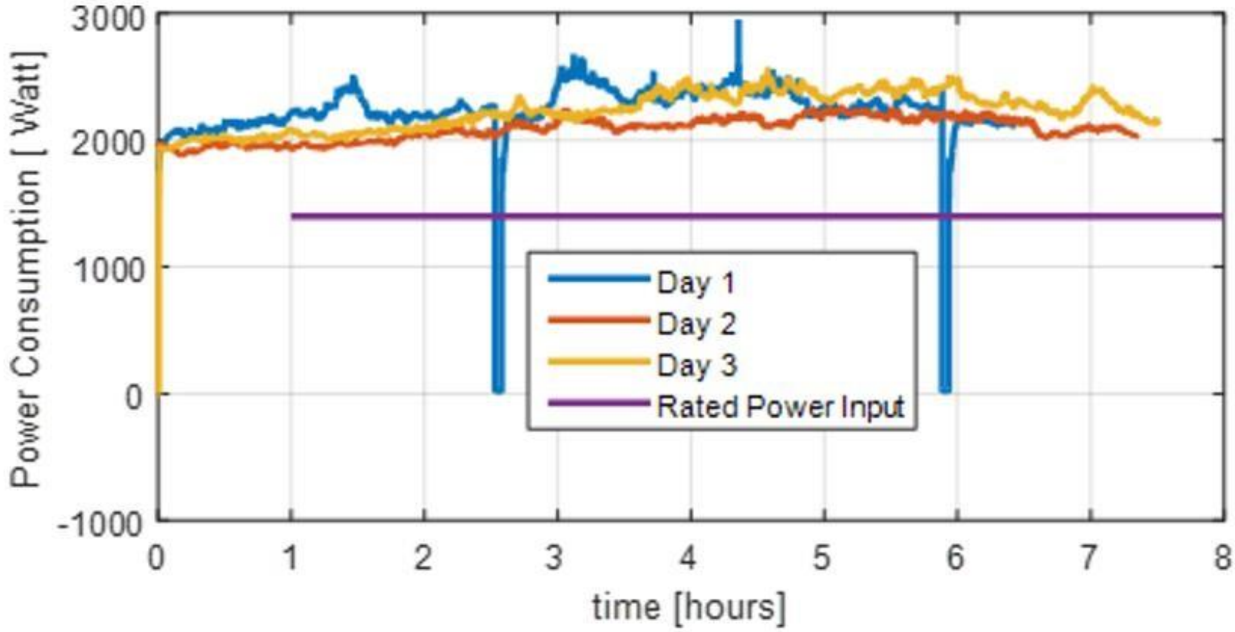

Figure 4.3 Power consumption of Chigo air-conditioner over a period

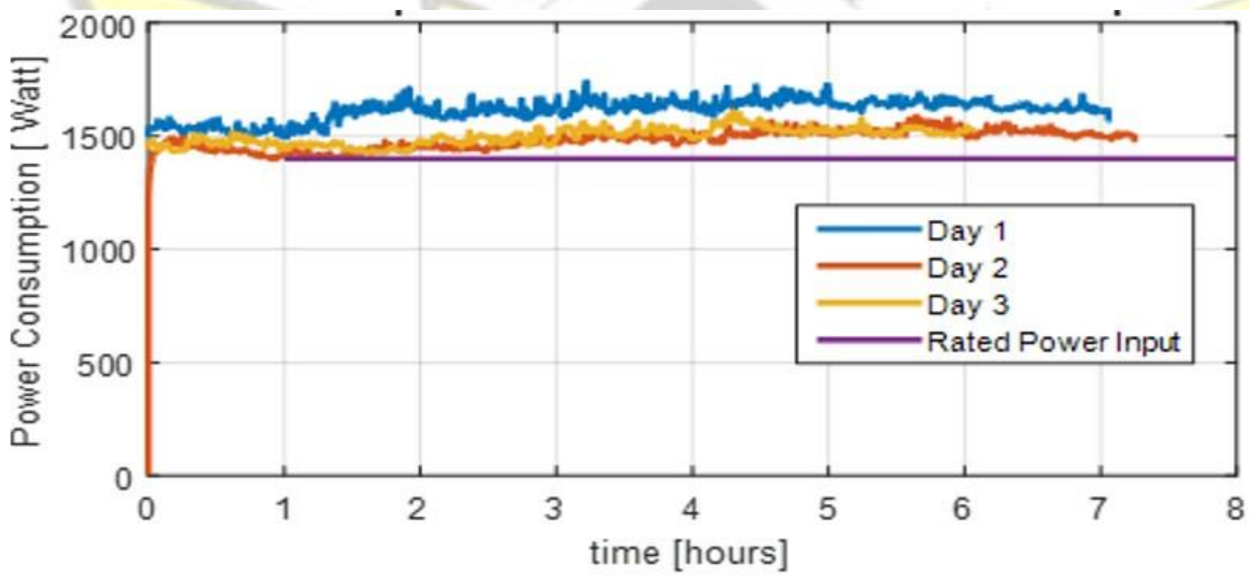

Figure 4.4 Power consumption of Chigo air-conditioner over a period

It is observed that 2850 W and 2000 W are the maximum and minimum measured power consumption rates respectively. This air-conditioner is at the Metrology lab, KNUST. The measured average power consumed is 2200 W. The maximum measured power consumed by the air-conditioner as shown in Figure 4.4 which is located at the MSc. Mechanical Engineering lecture room is about 1650 W. The minimum value measured is 1500 W with the average being 1530 W. It is important to mention that the power consumption measured at the MSc Mechanical lecture room was at no load conditions. This means there were no occupants in the room during the period the data was taken.

It should, however, be noted that even though both the Metrology and MSc. Lecture room airconditioners are of the same brand and specifications, their measured power consumptions are not the same. This is partly due to the frequency of opening and closing of the entrance door and also the various activities that take place in the two rooms.

Figure 4.5 shows a comparison of the average measured power consumption and the actual rated power input which is obtained from the name plate specifications of the four air-conditioners.

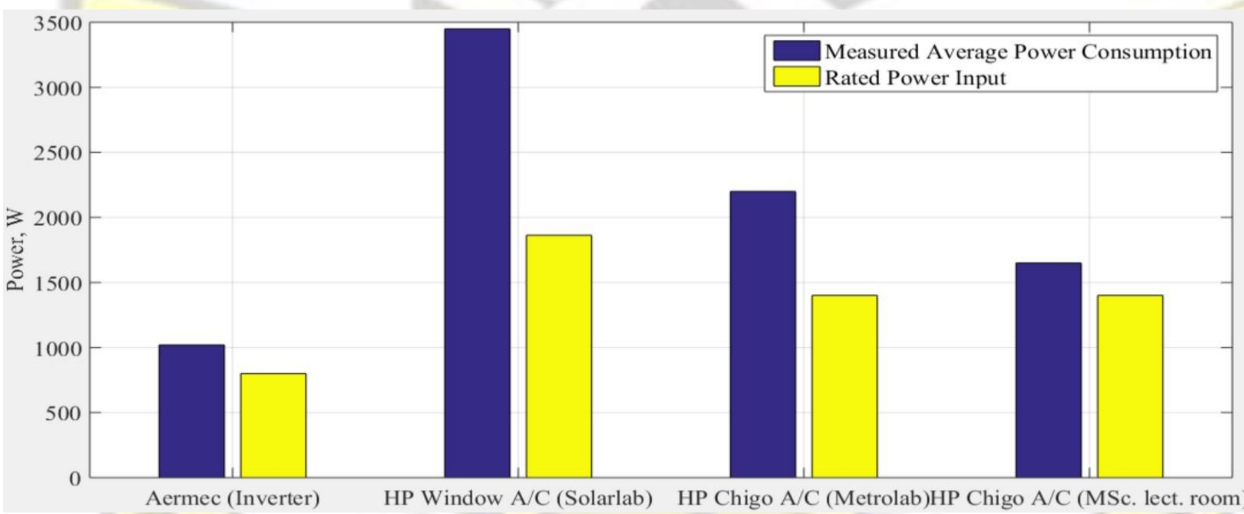

Figure 4.5 Comparison of the average power consumption and the rated power input of some selected air-conditioners

It is evident from Figure 4.5 that the rated power inputs of all four air-conditioners are less than the measured power consumption. This may be due to factors such as, the design operating conditions of the air-conditioners, that is, the climatic conditions. Ghana and therefore Kumasi is highly humid, therefore requiring cooling below the dew point temperature to remove moisture (latent) before reheating to the desired room temperature. This results in higher power consumption of the air-conditioners.

4.1.4 Estimated Cooling Load of the Air-Conditioners

Using the average power consumptions measured for the four air-conditioners, their average cooling loads are estimated from equation (4.1) using the energy efficiency ratings (EER) as shown in Figure 4.6.

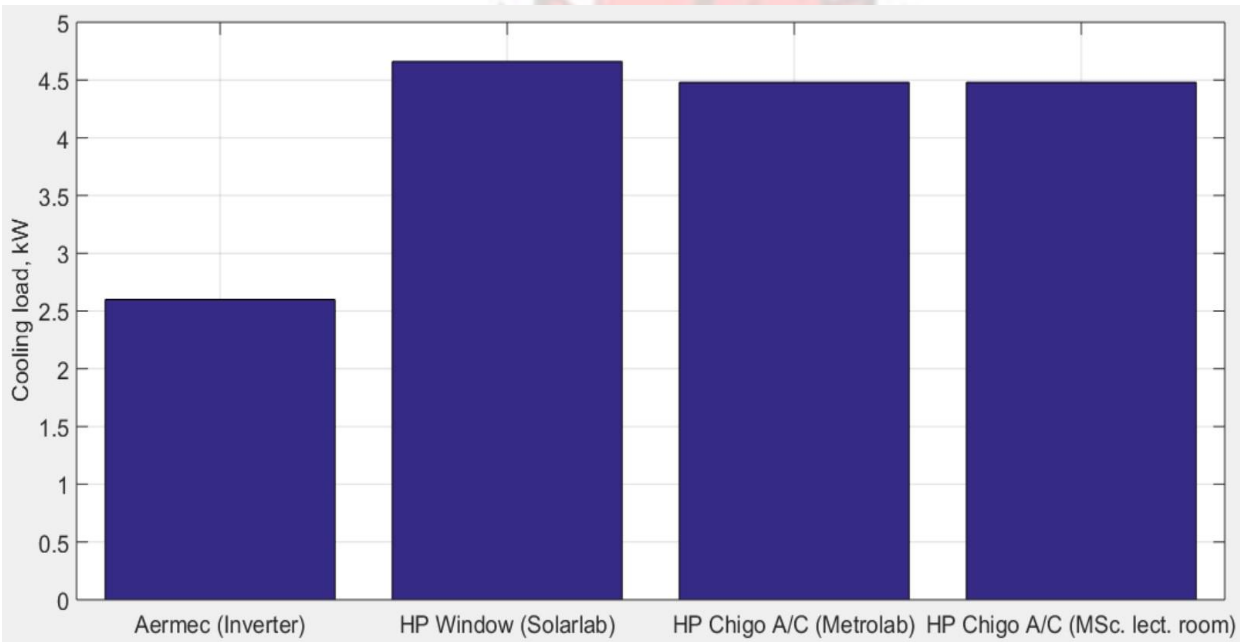

Figure 4.6 Estimated cooling load of the four air-conditioners

The Aermec (inverter) air-conditioner is seen to have the lowest cooling load of about 2.66 kW whiles the HP Window type at the solarlab (White-Westinghouse) having the highest cooling load of about 4.67 kW. This makes the Aermec air-conditioner the most efficient, hence having the highest energy efficiency rating (EER) as indicated on the air-conditioner's name plate

$Q^{cooling}$

EER= ______________ **(4.1)** *Powerconsumption*

4.2: Desiccant Cooling Air-Conditioning System ***4.2.1 Simulation of the Variation of Different Humidity Ratios of the Desiccant Cooling System***

Variations in humidity ratio of process air, ambient air, supply air, and room air versus time, are shown in Figure 4.7.

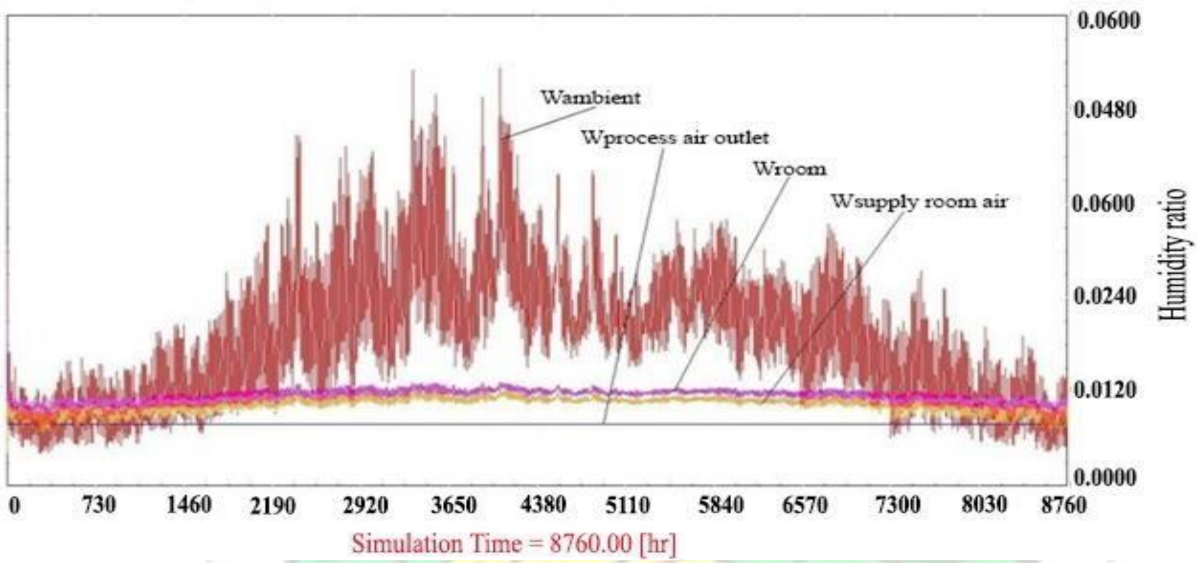

Figure 4.7 TRNSYS Simulation of humidity ratio variations of the desiccant cooling system on an annual basis

Humidity ratio is the main parameter indicating the removal of moisture from the room in terms of latent load from the desiccant cooling system especially in hot and humid climates to obtain desired comfort conditions inside the room. It is observed that the humidity ratio is by far higher in the ambient air. At the exit of the desiccant wheel ($W_{process\ air\ outlet}$), which is the process air outlet humidity ratio, there is a significant drop in the humidity ratio from about 0.052 kg/kg to about 0.008kg/kg as shown in Figure 4.7. Hence, there has been a reduction of about 83.62% of the outlet humidity ratio of the dehumidifier/desiccant wheel. Therefore, less energy is required to process supply air and room air since only sensible load occurs in the evaporative cooler. With the temperature and humidity ratios after the desiccant cooling system, the results of the potential reduction of the cooling load and also the potential reduction in the power consumption are presented in Figure 4.9 and Figure 4.10

4.2.2 Simulation of the Variation of Different Temperatures of the Desiccant Cooling System

Figure 4.8 shows simulation results for variation of temperatures in recirculation mode of the desiccant cooling system.

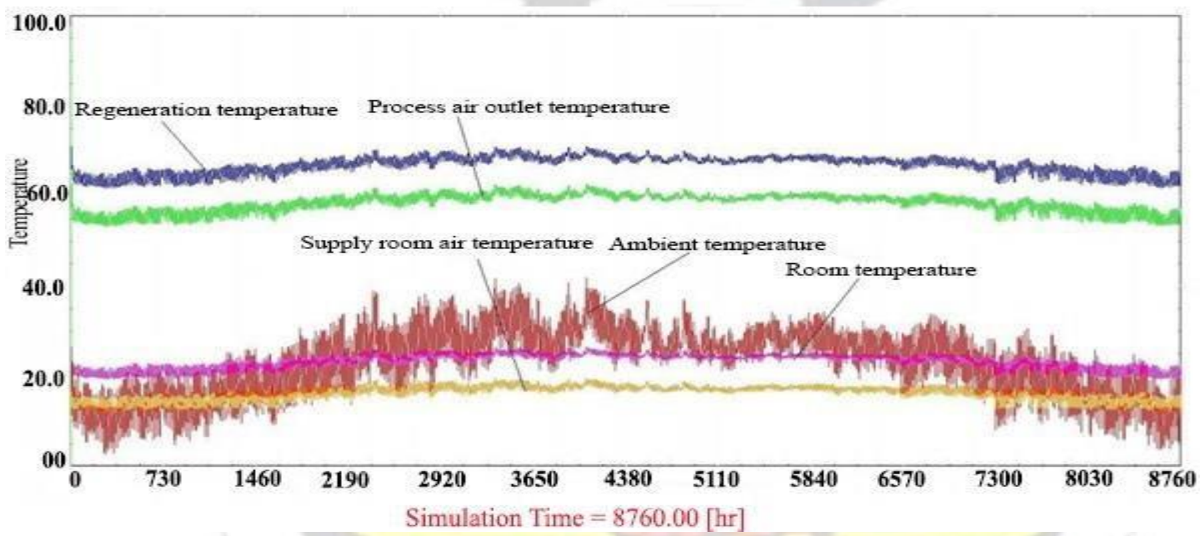

Figure 4.8 TRNSYS Simulation of temperature variations of the desiccant cooling system on an annual basis

It is observed that the required regeneration temperature for recirculation mode is about 64□C. Therefore, lower energy is needed in the heater to obtain the required regeneration air temperature for desorption of desiccant wheel. Variations in ambient temperature, Supply air temperature, process air outlet temperature and room temperature are also shown in Figure 4.8. The process air temperature at the outlet of the desiccant wheel increased as a result of removal of moisture from the ambient air during the dehumidification (desiccant removal) process. Temperature of supply air is about 16C after evaporative cooling, whereas the room temperature is seen to be 21C.

4.2.3 Potential Reduction of Cooling Load after Desiccant

From the variations in temperatures and humidity ratios results obtained from the analysis of the desiccant air-conditioning system simulated in TRNSYS, the reduction of the cooling load is calculated. This is done using equations (3.2) and (3.3) which is the cooling load equations for latent load and sensible load respectively.

Figure 4.9 shows the comparison of the estimated cooling loads of the four air-conditioners and the cooling loads after simulation of the desiccant air-conditioning system. Though the estimated cooling loads of the four air-conditioners differ, their cooling loads after desiccant are almost the same at approximately 1.65 kW as shown in Figure 4.9. This is due to the effectiveness of the desiccant in removing moisture in the air to be processed. There has been a significant reduction of the cooling loads for all the air-conditioners after using the desiccant. The highest reduction, 64.59% occurred in the HP Window air-conditioner (White-Westinghouse). The Aermec airconditioner has the lowest reduction of about 25.68% as it is already an efficient air-conditioner.

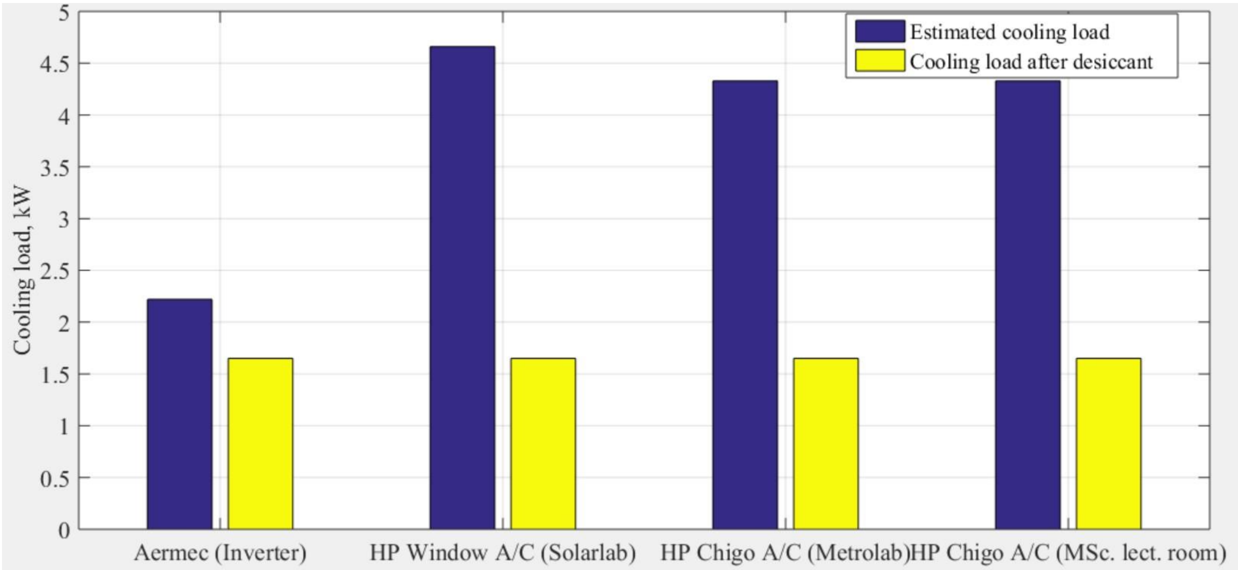

Figure 4.9 Comparison of the estimated cooling loads and the cooling loads after desiccant of the four air-conditioners

4.2.4 Potential Reduction in Electricity Consumption of the Air-Conditioners with Desiccant System.

Figure 4.10 shows a comparison of the estimated electricity consumption of the selected airconditioners using the power consumption values measured with the Fluke 345 energy meter, and the electricity consumption as calculated from the TRNSYS simulation when desiccant has been used to remove moisture before the air-conditioning process.

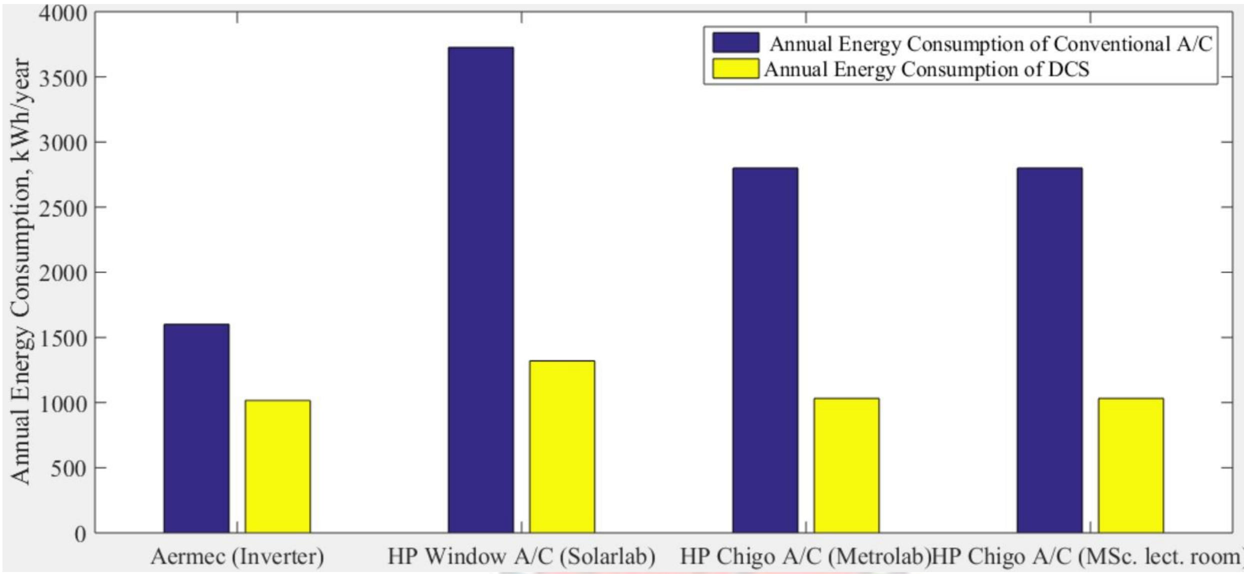

Figure 4.10 Annual energy consumption of conventional A/C and energy consumption of DCS

With the cooling loads after desiccant, the power consumptions are obtained using equation (4.1). This is compared with the measured average energy consumption of the conventional airconditioners as shown in Figure 4.10. It is observed that, there has been a drastic reduction in the energy consumption of all the air-conditioners. A potential reduction of about 584 kWh/year is obtained representing about 36.5% in the Aermec air-conditioner. Furthermore, HP Window type air-conditioner is observed to have the highest reduction of approximately 64.6%.

From the results obtained in the study, the conclusions and recommendations made are presented in the next chapter (chapter five).

CHAPTER FIVE: CONCLUSION AND RECOMMENDATION

5.1 Conclusions

In the present research work, measured data of some selected air-conditioners on KNUST Campus have been collected. Desiccant air-conditioning system has been modelled and simulated in TRNSYS software based on the weather data for Kumasi. Analysis has been performed on the data of both systems (air-conditioners without desiccant and one with desiccant). Results obtained from both systems have been presented to compare the potential reduction on the energy consumption of air-conditioners when desiccant is used which is the main goal of this thesis. The findings and conclusions of the research work are presented below based on the specific objectives outlined in this thesis.

1. The electricity consumption of some selected air-conditioners without desiccant system were measured using Fluke 345 Energy/Clamp Meter. The average electricity consumptions for the various air-conditioners have been measured successfully as 1.02 kW, 3.500 kW, 2.200 kW, and 1.5300 kW for the inverter air-conditioner, window airconditioner and the two split type air-conditioners respectively. It was observed from the analysis that the Aermec air-conditioner (inverter type) had the lowest power consumption due to its efficient nature as implied from its name plate. The measured average values of the air –conditioners were, however, higher than the name plate specifications, which are 0.8 kW, 1.863 kW, and 1.4 kW. This difference is due to the conditions under which the air-conditioners operate.
2. A desiccant air-conditioning system has been simulated using TRNSYS Software. The desiccant wheel takes care of the latent component of the load by removing moisture from the process air before finally entering the conditioned space. After air went through the

dehumidifier, there was significant drop in the humidity ratio 0.044 kg/kg (83.62%). This enabled less energy to be consumed since the latent part has already been accounted for.

3. The cooling loads for both the conventional air-conditioner without desiccant as well as the simulated desiccant system were compared. The results indicate that, a significant reduction of the cooling loads are observed in the desiccant cooling system. This is due to the fact that desiccant handles only the latent load which is very high in hot humid climates such as Ghana. The conventional air-conditioners cooling load was high since it first has to cool the air below its dew point to be able to condense to remove the latent load and further reheat to the desired temperature. Overall, the result shows that the highest reduction in the cooling load was 65% representing a huge savings.
4. The electricity consumption of the air-conditioners with desiccant cooling system have been determined, analysed and compared with the selected air-conditioners without desiccant cooling system. The results show a phenomenal increase in the savings of energy consumption after the application of the desiccant system. A compelling 64.6% and 36.5% annual savings were observed as the highest and lowest of the air-conditioners respectively.

5.2 Recommendations

The following recommendations are suggested based on the outcome of the results.

1. The simulated desiccant system was only compared with measured data of some selected air-conditioners. It is recommended that a desiccant system be constructed and installed for experimental data to be taken and compared with the simulation model.
2. The system can be improved by investigating it within a multi-zone building and real control systems to make it more close to real applications.

REFERENCES

A.S.H.R.A.E Fundamentals (2009) *American society of heating, refrigerating and airconditioning engineers, Handbook, ASHRAE Fundamentals,*. SI Edition. Atlanta, Ga.

Ahmed, M. A. *et al.* (2017) 'Thermodynamic analysis of an innovative liquid desiccant air conditioning system to supply potable water', *Energy Conversion and Management*. Elsevier Ltd, 148, pp. 161–173. doi: 10.1016/j.enconman.2017.05.049.

Al-waked, R. *et al.* (2013) 'CFD simulation of air to air enthalpy heat exchanger', *Energy Conversion and Management*. Elsevier Ltd, 74, pp. 377–385. doi: 10.1016/j.enconman.2013.05.038.

Angrisani, G., Roselli, C. and Sasso, M. (2015) 'Experimental assessment of the energy performance of a hybrid desiccant cooling system and comparison with other air-conditioning technologies', *Applied Energy*. Elsevier Ltd, 138, pp. 533–545. doi: 10.1016/j.apenergy.2014.10.065.

Aryal, P. and Leephakpreeda, T. (2015) *CFD Analysis on Thermal Comfort and Energy Consumption Effected by Partitions in Air-Conditioned Building*, *Energy Procedia*. Elsevier B.V. doi: 10.1016/j.egypro.2015.11.459.

ASHRAE (2013) 'American Society of Heating, Refrigeration and Air-Conditioning Engineers', *Standard 55-2013: Thermal Environmental Conditions for Human Occupancy, 2013, doi :ISSN 1041-2336.*

Chauhan, S. S. and Rajput, S. P. S. (2016) 'Parametric analysis of a combined dew point evaporative-vapour compression based air conditioning system', *Alexandria Engineering Journal*. Faculty of Engineering, Alexandria University, 1, pp. 1–12. doi: 10.1016/j.aej.2016.05.005.

Dai, Y., Li, X. and Wang, R. (2015) 'Theoretical Analysis and Case Study on Solar Driven Twostage Rotary Desiccant Cooling System Combined with Geothermal Heat Pump', *Energy Procedia*. Elsevier B.V., 70, pp. 418–426. doi: 10.1016/j.egypro.2015.02.143.

Du, Z., Jin, X. and Fan, B. (2015) 'Evaluation of operation and control in HVAC (heating , ventilation and air conditioning) system using exergy analysis method', *Energy*. Elsevier Ltd, pp. 1–10. doi: 10.1016/j.energy.2015.05.119.

Gandhidasan, P. (2005) 'Quick performance prediction of liquid desiccant regeneration in a packed bed', 79, pp. 47–55. doi: 10.1016/j.solener.2004.10.002.

Ge, G., Xiao, F. and Niu, X. (2011) 'Control strategies for a liquid desiccant air-conditioning system', *Energy & Buildings*. Elsevier B.V., 43(6), pp. 1499–1507. doi: 10.1016/j.enbuild.2011.02.011.

Ghazikhani, M., Khazaee, I. and Vahidifar, S. (2016) 'Exergy analysis of two humidification process methods in air-conditioning systems', *Energy & Buildings*. Elsevier B.V., 124, pp. 129–140. doi: 10.1016/j.enbuild.2016.04.077.

Hamed, A. M. and Awad, M. M. (2011) 'Experimental investigation on the performance of radial fl ow desiccant bed using activated alumina', *Applied Thermal Engineering*. Elsevier Ltd, 31(14–15), pp. 2709–2715. doi: 10.1016/j.applthermaleng.2011.04.041.

Heidarinejad, G. and Pasdarshahri, H. (2010) 'The effects of operational conditions of the desiccant wheel on the performance of desiccant cooling cycles', *Energy and Buildings*. Elsevier B.V., 42(12), pp. 2416–2423. doi: 10.1016/j.enbuild.2010.08.011.

Hürdoğan, E. *et al.* (2013) 'Experimental exergoeconomic assessment of a desiccant cooling system', *Energy Conversion and Management*, 69, pp. 9–16. doi: 10.1016/j.enconman.2013.01.009.

Jagirdar, M., Lee, P. S. and Ho, G. W. (2017) 'Feasibility Study of a Parallel Plate Desiccant Coated Heat and Mass Regenerator for Dehumidification', *Energy Procedia*. The Author(s), 105, pp. 5034–5039. doi: 10.1016/j.egypro.2017.03.1011.

Jani, D. B., Mishra, M. and Sahoo, P. K. (2016) 'Experimental investigation on solid desiccant – vapor compression hybrid air-conditioning system in hot and humid weather', *Applied Thermal Engineering*. Elsevier Ltd, 104, pp. 556–564. doi: 10.1016/j.applthermaleng.2016.05.104.

Jia, C. X. *et al.* (2006) 'Analysis on a hybrid desiccant air-conditioning system', 26, pp. 2393–2400. doi: 10.1016/j.applthermaleng.2006.02.016.

Jiang, Y. *et al.* (2014) 'Experimental investigation on a novel temperature and humidity independent control air conditioning system e Part I : Cooling condition', 73, pp. 782–791. doi: 10.1016/j.applthermaleng.2014.08.028.

Kabeel, A. E. (2007) 'Solar powered air conditioning system using rotary honeycomb desiccant wheel', *Renewable Energy*, 32(11), pp. 1842–1857. doi: 10.1016/j.renene.2006.08.009.

Longo, G. A. and Gasparella, A. (2005) 'Experimental and theoretical analysis of heat and mass transfer in a packed column dehumidifier / regenerator with liquid desiccant', 48, pp. 5240–5254. doi: 10.1016/j.ijheatmasstransfer.2005.07.011.

Luo, Y., Yang, H., *et al.* (2016) 'Application of CFD Model in Analyzing the Performance of a Liquid Desiccant Dehumidifier', *Energy Procedia*. Elsevier B.V., 88, pp. 491–497. doi: 10.1016/j.egypro.2016.06.068.

Luo, Y., Chen, Y., *et al.* (2016) 'Study on an internally-cooled liquid desiccant dehumidifier with CFD model q', *Applied Energy*. Elsevier Ltd. doi: 10.1016/j.apenergy.2016.05.133.

Luo, Y., Yang, H. and Lu, L. (2013) 'Liquid desiccant dehumidifier : Development of a new performance predication model based on CFD', *International Journal of Heat and Mass Transfer*. Elsevier Ltd, 69, pp. 408–416. doi: 10.1016/j.ijheatmasstransfer.2013.10.033.

Martin, V. and Goswami, D. Y. (2011) 'Effectiveness of Heat and Mass Transfer Processes in a Packed Bed Liquid Desiccant Dehumidifier / Regenerator Effectiveness of Heat and Mass Transfer Processes in a Packed Bed Liquid Desiccant Dehumidifier / Regenerator', 9669, pp. 20–39.

Mei, L. and Dai, Y. J. Ã. (2008) 'A technical review on use of liquid-desiccant dehumidification for air-conditioning application', 12, pp. 662–689. doi: 10.1016/j.rser.2006.10.006.

Mosaffa, A. H. *et al.* (2014) 'Advanced exergy analysis of an air conditioning system incorporating thermal energy storage', *Energy*. Elsevier Ltd, pp. 1–8. doi: 10.1016/j.energy.2014.10.006. Oberg, V. and Goswami, D. Y. (1998) 'Experimental Study of the Heat and Mass Transfer in a Packed Bed Liquid Desiccant Air Dehumidifier', (November 1998), pp. 289–297.

Opoku, R., Mensah-Darkwa, K. and Samed Muntaka, A. (2018) 'Techno-economic analysis of a hybrid solar PV-grid powered air-conditioner for daytime office use in hot humid climates – A case study in Kumasi city, Ghana', *Solar Energy*. Elsevier, 165(February), pp. 65–74. doi: 10.1016/j.solener.2018.03.013.

Owusu-achaw, Kwame, Bimpong, H. (2017) *Refrigeration and Air Conditioning Greenhouse Gas Inventory DRAFT Report for Ghana*.

Rosen, M. A. and Dincer, I. (2003) 'Thermoeconomic analysis of power plants: An application to a coal fired electrical generating station', *Energy Conversion and Management*, 44(17), pp. 2743–2761. doi: 10.1016/S0196-8904(03)00047-5.

Th, A. *et al.* (2013) 'Survey of hybrid liquid desiccant air conditioning systems', *Renewable and Sustainable Energy Reviews*. Elsevier, 20, pp. 186–200. doi: 10.1016/j.rser.2012.11.065.

Uçkan, I., Yılmaz, Tuncay, E. H. and Büyükalaca, O. (2014) 'Exergy analysis of a novel configuration of desiccant based evaporative air conditioning system', 84, pp. 524–532. doi: 10.1016/j.enconman.2014.05.006.

Xiao-xia, X. I. A., Zhi-qi, W. and Shun-sheng, X. U. (2012) 'Exergy Analysis of Energy Consumption for Primary Return Air Conditioning System', 24, pp. 2131–2137. doi: 10.1016/j.phpro.2012.02.313.

Youssef, A. A. *et al.* (2017) 'Studying comfort in a room with cold air system using computational fluid dynamics', *Ain Shams Engineering Journal*. Ain Shams University. doi: 10.1016/j.asej.2016.07.005.

Zhang, F., Yin, Y. and Zhang, X. (2017) ‘Performance analysis of a novel liquid desiccant evaporative cooling fresh air conditioning system with solution recirculation’, *Building and Environment*. Elsevier Ltd, 117, pp. 218–229. doi: 10.1016/j.buildenv.2017.03.015.

Zhang, Z., Liu, S. and Tian, L. (2011) ‘Thermodynamic analysis of air cycle refrigeration system for Chinese train air conditioning’, 1, pp. 16–22. doi: 10.1016/j.sepro.2011.08.004.

APPENDICES

APPENDIX A

SAMPLE CONNECTION WINDOW OF VARIOUS COMPONENTS OF THE DESICCANT COOLING SYSTEM USED IN THE THESIS

Humidity ratio	Process Air Inlet Temperature	30
Wet bulb temperature	Process Air Inlet Humidity Ratio	0.007
Enthalpy	Process Air % Relative Humidity	99.0
Density of mixture	Process Air Flowrate	1000
Density of dry air	Process Air Inlet Pressure	1.00
Percent relative humidity	Process Air Pressure Drop	0.
Dry bulb temperature	Regeneration Air Inlet Temperature	71
Dew point temperature.	Regeneration Air Humidity Ratio	0.01428
Status	Regeneration Air % Relative Humidity	50
Atmospheric pressure	Regeneration Air Flowrate	500
	Regeneration Air Inlet Pressure	1
	Regeneration Air Pressure Drop	0.
	Control Signal	1

Sample connection window between psychrometric and desiccant wheel (dehumidifier)

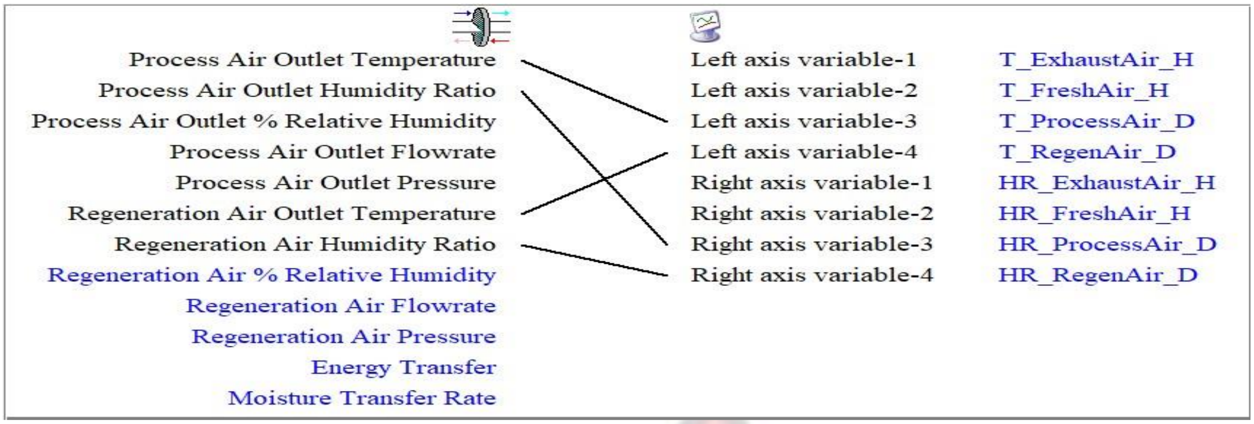

Sample connection window between desiccant wheel (dehumidifier) and online plotter

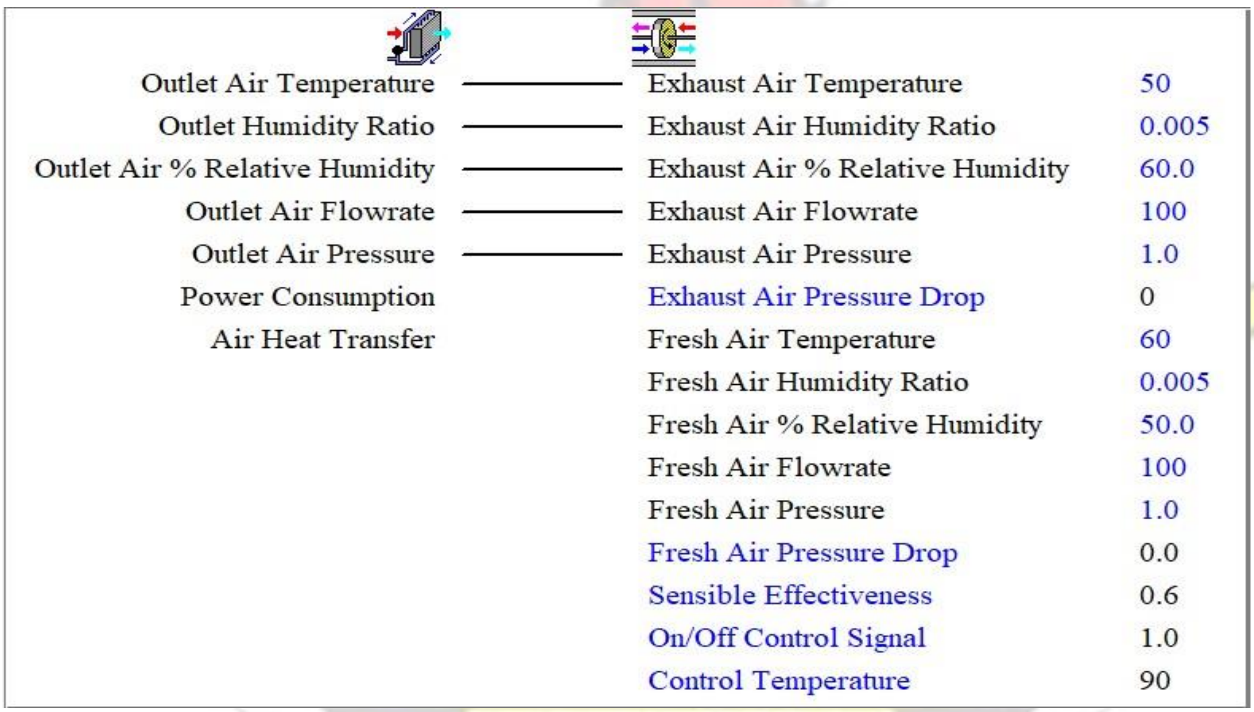

Sample connection window between evaporative cooler and heat wheel

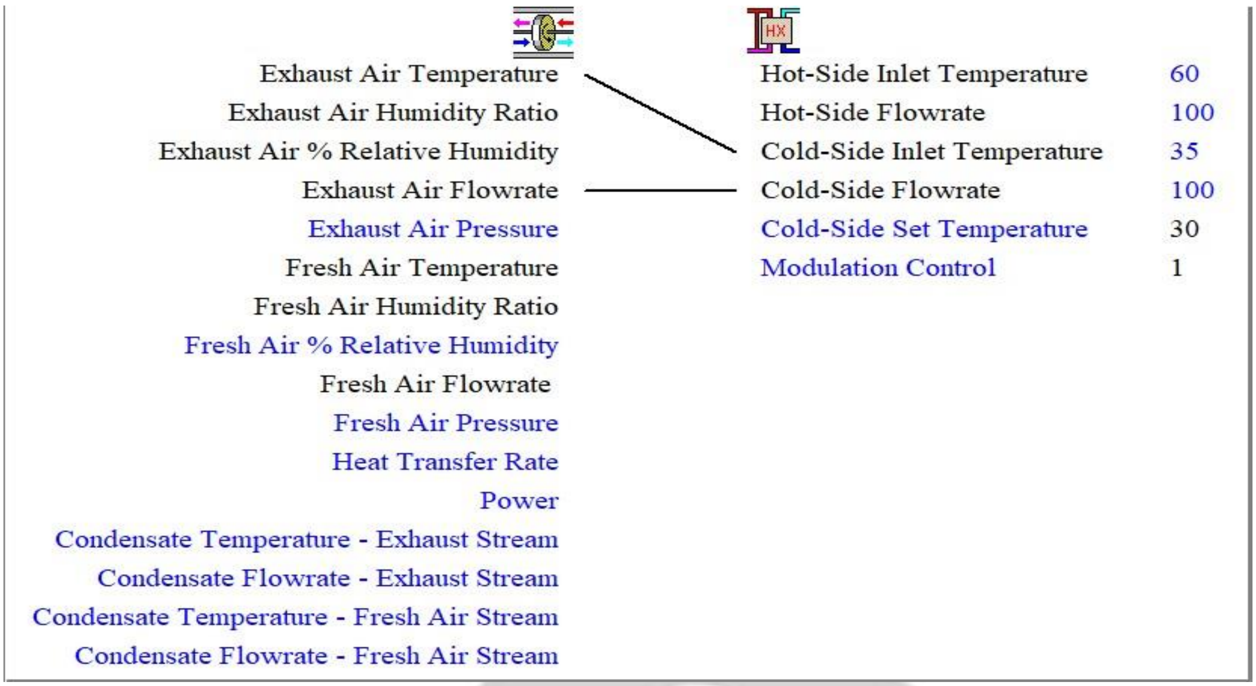

Sample connection window between heat wheel and heat exchanger

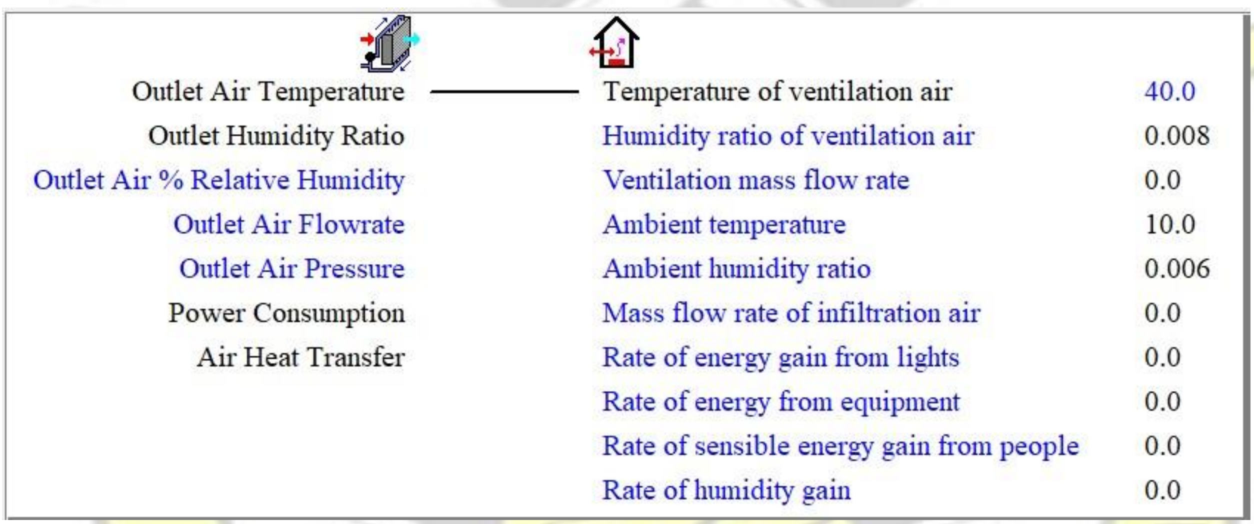

Sample connection window between evaporative cooler and building

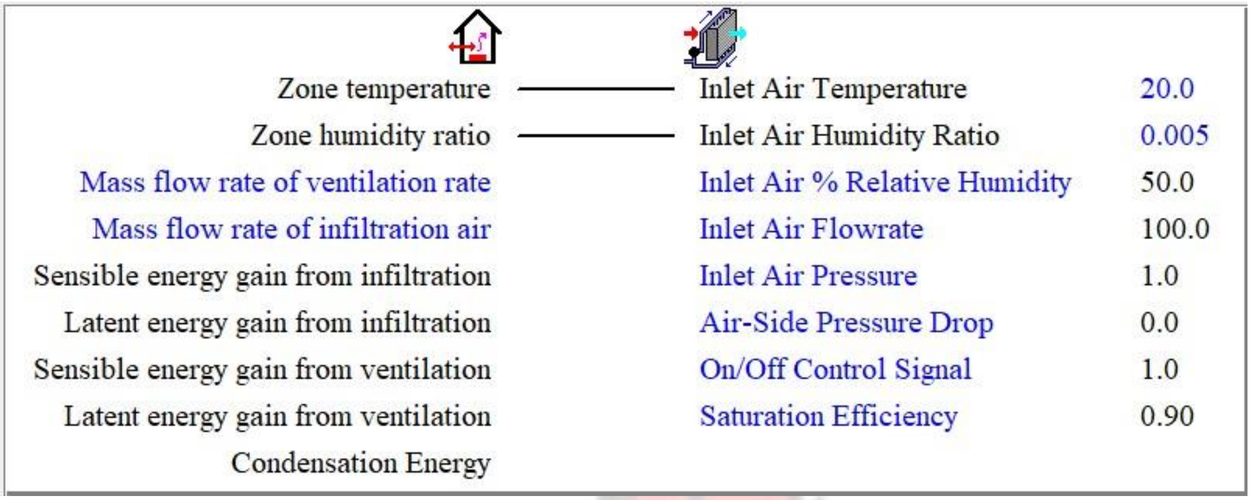
Zone temperature
Inlet Air Temperature
20.0
Zone humidity ratio
Inlet Air Humidity Ratio
0.005
Mass flow rate of ventilation rate
Inlet Air % Relative Humidity
50.0
Mass flow rate of infiltration air
Inlet Air Flowrate
100.0
Sensible energy gain from infiltration
Inlet Air Pressure
1.0
Latent energy gain from infiltration
Air-Side Pressure Drop
0.0
Sensible energy gain from ventilation
On/Off Control Signal
1.0
Latent energy gain from ventilation
Saturation Efficiency
0.90
Condensation Energy

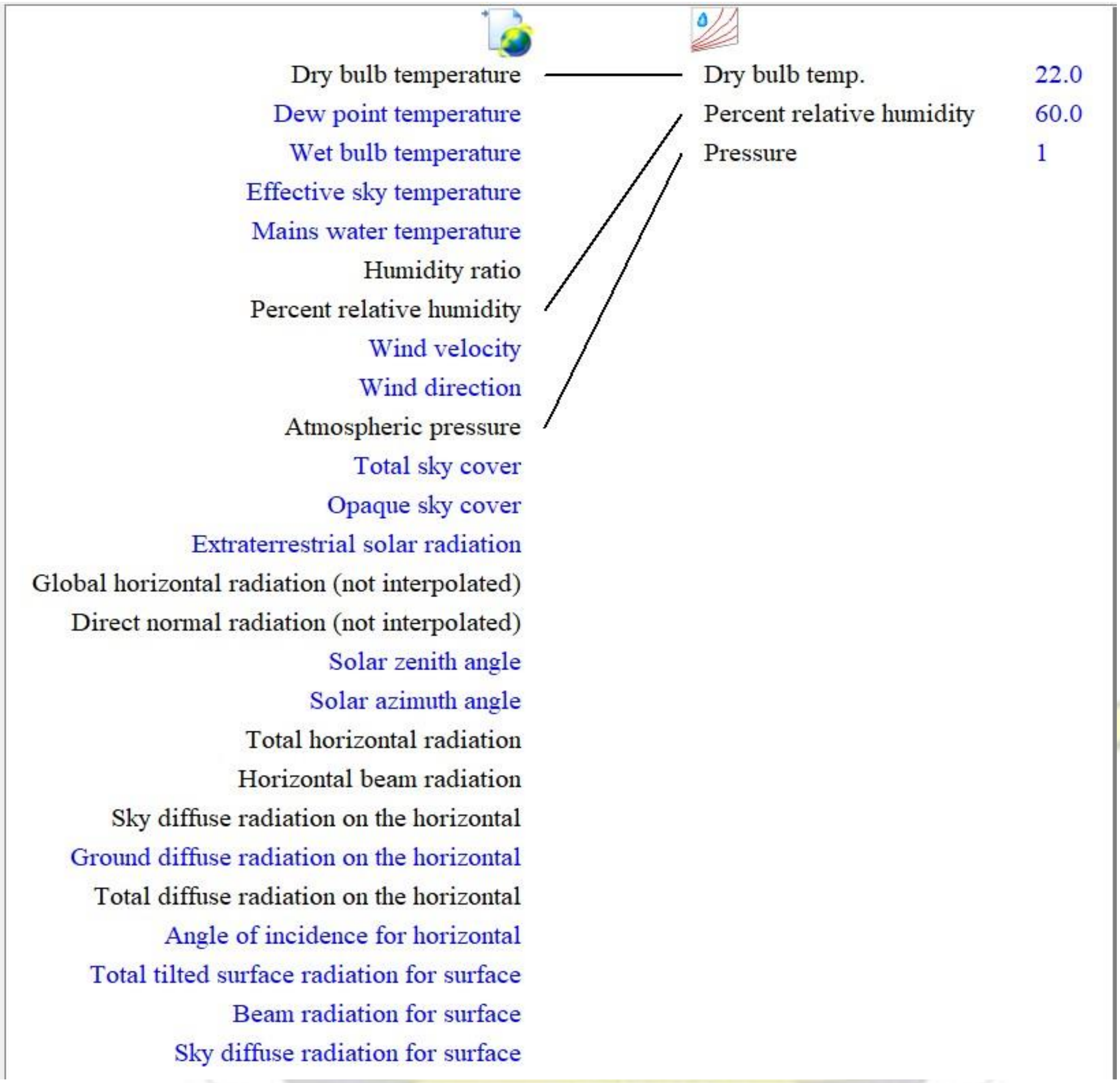
Dry bulb temperature
Dew point temperature
Wet bulb temperature
Effective sky temperature
Mains water temperature
Humidity ratio
Percent relative humidity
Wind velocity
Wind direction
Atmospheric pressure
Total sky cover
Opaque sky cover
Extraterrestrial solar radiation
Global horizontal radiation (not interpolated)
Direct normal radiation (not interpolated)
Solar zenith angle
Solar azimuth angle
Total horizontal radiation
Horizontal beam radiation
Sky diffuse radiation on the horizontal
Ground diffuse radiation on the horizontal
Total diffuse radiation on the horizontal
Angle of incidence for horizontal
Total tilted surface radiation for surface
Beam radiation for surface
Sky diffuse radiation for surface
Dry bulb temp. 22.0
Percent relative humidity 60.0
Pressure 1

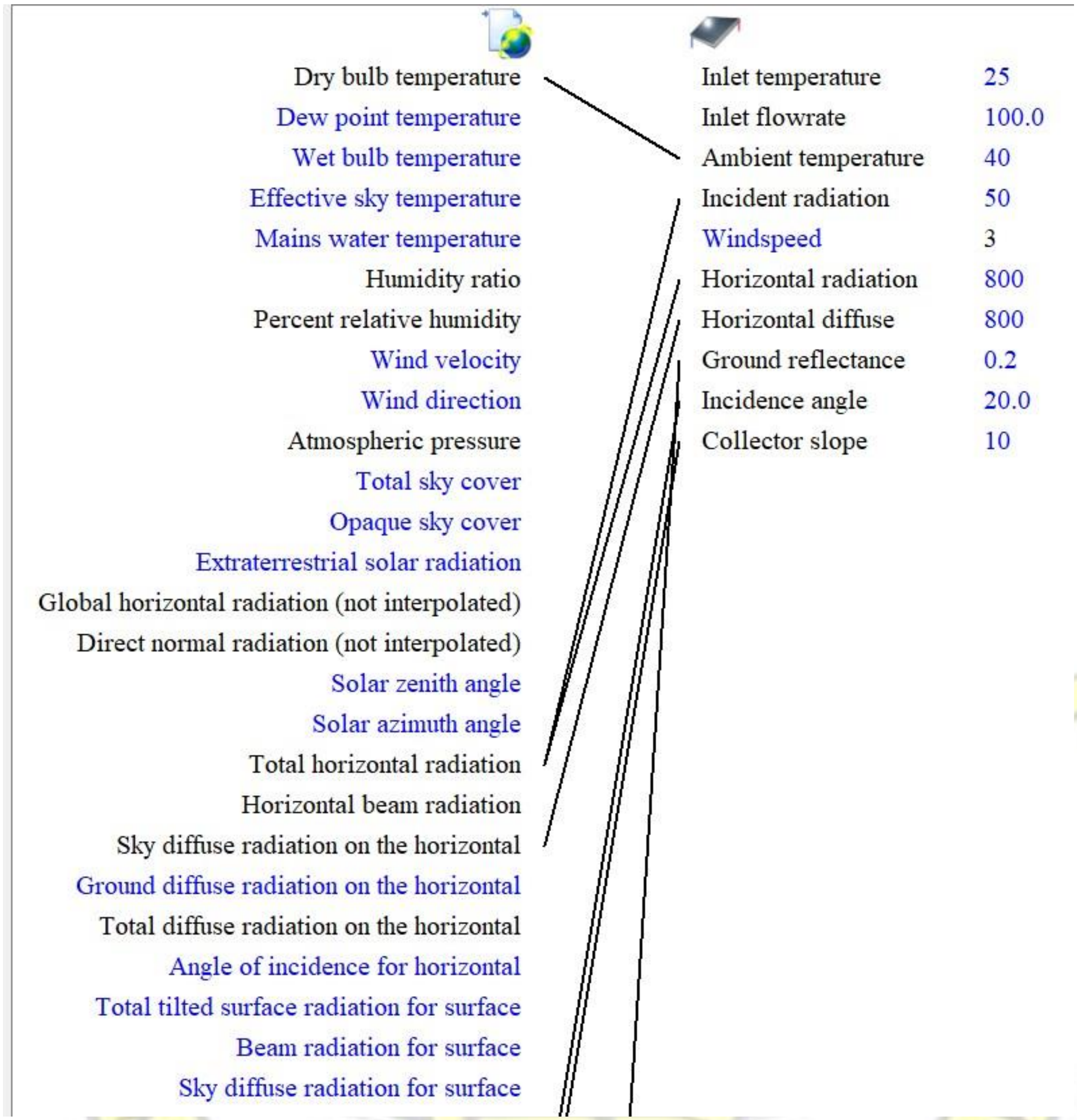

Sample connection window between weather data and solar thermal collector

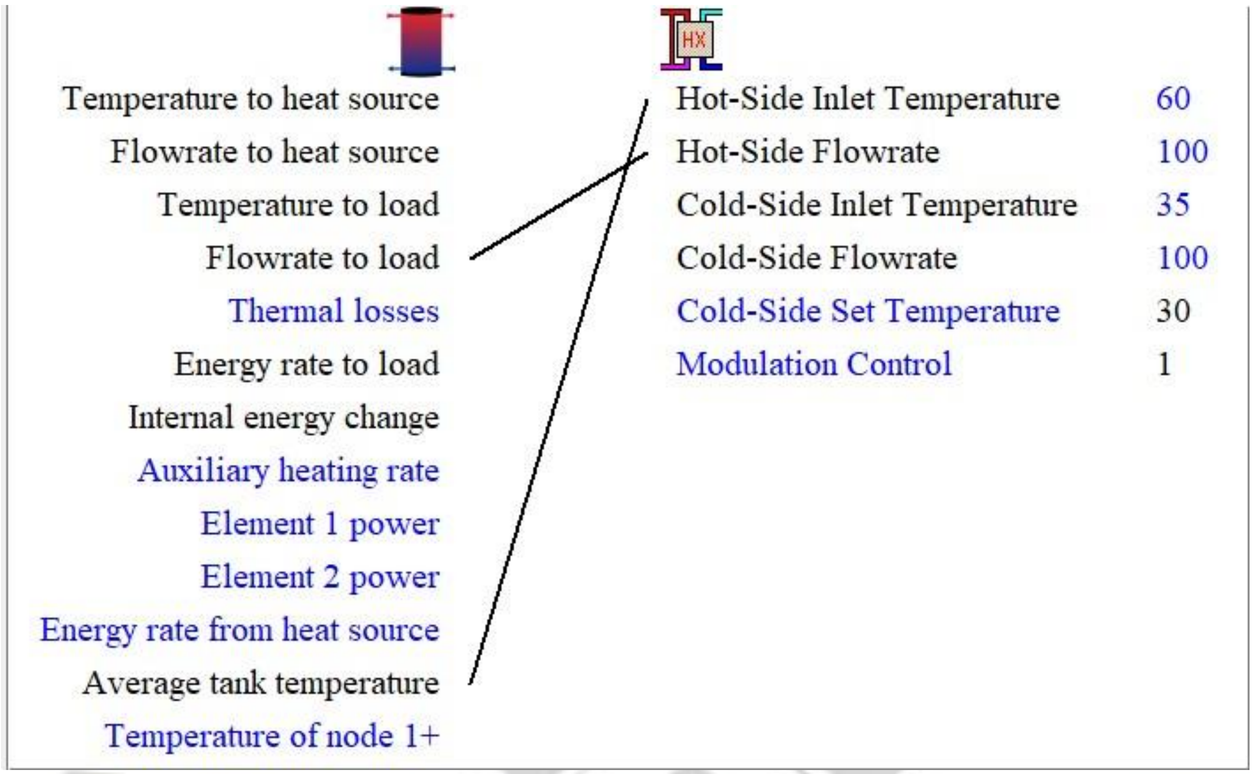
Temperature to heat source
Flowrate to heat source
Temperature to load
Flowrate to load
Thermal losses
Energy rate to load
Internal energy change
Auxiliary heating rate
Element 1 power
Element 2 power
Energy rate from heat source
Average tank temperature
Temperature of node 1+
HX
Hot-Side Inlet Temperature 60
Hot-Side Flowrate 100
Cold-Side Inlet Temperature 35
Cold-Side Flowrate 100
Cold-Side Set Temperature 30
Modulation Control 1

APPENDIX B

PARAMETER, INPUT AND OUTPUT WINDOWS OF THE VARIOUS COMPONENTS OF THE DESICCANT COOLING SYSTEM

Parameter | Input | Output | Derivative | Special Cards | External Files | Comment

	Name	Value	Unit	More	Macro
1	Building loss coefficient	5	kJ/hr.m^2.K	More...	☑
2	Building capacitance	1000.0	kJ/K	More...	☑
3	Specific heat of building air	1.007	kJ/kg.K	More...	☑
4	Density of building air	1.2	kg/m^3	More...	☑
5	Building surface area	100	m^2	More...	☑
6	Building volume	200.0	m^3	More...	☑
7	Humidity ratio multiplier	1	-	More...	☑
8	Initial temperature	20	C	More...	☑
9	Initial humidity ratio	0.005	-	More...	☑
10	Latent heat of vaporization	2260	kJ/kg	More...	☑

Parameter window sample of the building used

Parameter | Input | Output | Derivative | Special Cards | External Files | Comment

	Name	Value	Unit	More	Macro
1	Temperature of ventilation air	40.0	C	More...	☑
2	Humidity ratio of ventilation air	0.008	-	More...	☑
3	Ventilation mass flow rate	0.0	kg/hr	More...	☑
4	Ambient temperature	10.0	C	More...	☑
5	Ambient humidity ratio	0.006	-	More...	☑
6	Mass flow rate of infiltration air	0.0	kg/hr	More...	☑
7	Rate of energy gain from lights	0.0	kJ/hr	More...	☑
8	Rate of energy from equipment	0.0	kJ/hr	More...	☑
9	Rate of sensible energy gain from people	0.0	kJ/hr	More...	☑
10	Rate of humidity gain	0.0	kg/hr	More...	☑

Input window sample of the building used

Parameter | Input | Output | Derivative | Special Cards | External Files | Comment

	Name	Value	Unit	More	Macro	Print
1	Zone temperature	0	C	More...	☑	☐
2	Zone humidity ratio	0	-	More...	☑	☐
3	Mass flow rate of ventilation rate	0	kg/hr	More...	☑	☐
4	Mass flow rate of infiltration air	0	kg/hr	More...	☑	☐
5	Sensible energy gain from infiltration	0	kJ/hr	More...	☑	☐
6	Latent energy gain from infiltration	0	kJ/hr	More...	☑	☐
7	Sensible energy gain from ventilation	0	kJ/hr	More...	☑	☐
8	Latent energy gain from ventilation	0	kJ/hr	More...	☑	☐
9	Condensation Energy	0	kJ/hr	More...	☑	☐

Output window sample of the building used

Building

Parameter | Input | Output | Derivative | Special Cards | External Files | Comment

		Name	Value	Unit	More	Macro
1		Humidity Mode	2	-	More...	☑
2		Rated Power	671.1	kJ/hr	More...	☑
3		Control Mode	1	-	More...	☑

Parameter window sample of the heat wheel

Parameter | Input | Output | Derivative | Special Cards | External Files | Comment

		Name	Value	Unit	More	Macro
1		Exhaust Air Temperature	50	C	More...	☑
2		Exhaust Air Humidity Ratio	0.005	-	More...	☑
3		Exhaust Air % Relative Humidity	60.0	-	More...	☑
4		Exhaust Air Flowrate	100	kg/hr	More...	☑
5		Exhaust Air Pressure	1.0	atm	More...	☑
6		Exhaust Air Pressure Drop	0	atm	More...	☑
7		Fresh Air Temperature	60	C	More...	☑
8		Fresh Air Humidity Ratio	0.005	-	More...	☑
9		Fresh Air % Relative Humidity	50.0	-	More...	☑
10		Fresh Air Flowrate	100	kg/hr	More...	☑
11		Fresh Air Pressure	1.0	atm	More...	☑

Input window sample of the heat wheel

Parameter | Input | Output | Derivative | Special Cards | External Files | Comment

		Name	Value	Unit	More	Macro	Print
1		Exhaust Air Temperature	20.0	C	More...	☑	☐
2		Exhaust Air Humidity Ratio	0.001	-	More...	☑	☐
3		Exhaust Air % Relative Humidity	50.0	-	More...	☑	☐
4		Exhaust Air Flowrate	0	kg/hr	More...	☑	☐
5		Exhaust Air Pressure	0	atm	More...	☑	☐
6		Fresh Air Temperature	20.0	C	More...	☑	☐
7		Fresh Air Humidity Ratio	0.001	-	More...	☑	☐
8		Fresh Air % Relative Humidity	50.0	-	More...	☑	☐
9		Fresh Air Flowrate	0.0	kg/hr	More...	☑	☐
10		Fresh Air Pressure	0	atm	More...	☑	☐
11		Heat Transfer Rate	0.0	kJ/hr	More...	☑	☐

Output window sample of the heat wheel

Parameter | Input | Output | Derivative | Special Cards | External Files | Comment

		Name	Value	Unit	More	Macro
1		Humidity Mode	2	-	More...	☑
2		Parasitic Power	**2**	**kW**	More...	☑

Parameter window sample of the evaporative cooler

Parameter | Input | Output | Derivative | Special Cards | External Files | Comment

		Name	Value	Unit	More	Macro
1		Inlet Air Temperature	20.0	C	More...	☑
2		Inlet Air Humidity Ratio	0.005	-	More...	☑
3		Inlet Air % Relative Humidity	50.0	-	More...	☑
4		Inlet Air Flowrate	100.0	kg/hr	More...	☑
5		Inlet Air Pressure	1.0	atm	More...	☑
6		Air-Side Pressure Drop	0.0	atm	More...	☑
7		On/Off Control Signal	1.0	-	More...	☑
8		Saturation Efficiency	0.90	-	More...	☑

Input window sample of the evaporative cooler

Parameter | Input | Output | Derivative | Special Cards | External Files | Comment

		Name	Value	Unit	More	Macro	Print
1		Outlet Air Temperature	*0*	C	More...	☑	☐
2		Outlet Humidity Ratio	*0*	-	More...	☑	☐
3		Outlet Air % Relative Humidity	*50.0*	-	More...	☑	☐
4		Outlet Air Flowrate	*0*	kg/hr	More...	☑	☐
5		Outlet Air Pressure	*0*	atm	More...	☑	☐
6		Power Consumption	*0*	kJ/hr	More...	☑	☐
7		Air Heat Transfer	*0*	kJ/hr	More...	☑	☐

Output window sample of the evaporative cooler